Lawrence Berkeley National Laboratory
Recent Work

Title
THE NMR RELAXATION MECHANISMS OF 017 IN AQUEOUS SOLUTIONS OF PARAMAGNETIC CATIONS AND THE LIFETIME OF WATER MOLECULES IN THE FIRST COORDINATION SPHERE

Permalink
https://escholarship.org/uc/item/2ch8j5gt

Author
Swift, Terrence James.

Publication Date
1962-05-01

eScholarship.org Powered by the California Digital Library
University of California

UCRL 10274

University of California

Ernest O. Lawrence Radiation Laboratory

THE NMR RELAXATION MECHANISMS OF O^{17} IN AQUEOUS SOLUTIONS OF PARAMAGNETIC CATIONS AND THE LIFETIME OF WATER MOLECULES IN THE FIRST COORDINATION SPHERE

TWO-WEEK LOAN COPY

This is a Library Circulating Copy which may be borrowed for two weeks. For a personal retention copy, call Tech. Info. Division, Ext. 5545

DISCLAIMER

This document was prepared as an account of work sponsored by the United States Government. While this document is believed to contain correct information, neither the United States Government nor any agency thereof, nor the Regents of the University of California, nor any of their employees, makes any warranty, express or implied, or assumes any legal responsibility for the accuracy, completeness, or usefulness of any information, apparatus, product, or process disclosed, or represents that its use would not infringe privately owned rights. Reference herein to any specific commercial product, process, or service by its trade name, trademark, manufacturer, or otherwise, does not necessarily constitute or imply its endorsement, recommendation, or favoring by the United States Government or any agency thereof, or the Regents of the University of California. The views and opinions of authors expressed herein do not necessarily state or reflect those of the United States Government or any agency thereof or the Regents of the University of California.

Research and Development

UCRL-10274
UC-4 Chemistry
TID-4500 (17th Ed.)

UNIVERSITY OF CALIFORNIA
Lawrence Radiation Laboratory
Berkeley, California

Contract No. W-7405-eng-48

THE NMR RELAXATION MECHANISMS OF O^{17} IN AQUEOUS SOLUTIONS OF PARAMAGNETIC CATIONS AND THE LIFETIME OF WATER MOLECULES IN THE FIRST COORDINATION SPHERE

Terrence James Swift

Thesis

May 1962

Reproduced by the Technical Information Division
directly from the author's copy

Printed in USA. Price $2.00. Available from the
Office of Technical Services
U. S. Department of Commerce
Washington 25, D.C.

THE NMR RELAXATION MECHANISMS OF O^{17} IN AQUEOUS SOLUTIONS OF PARAMAGNETIC CATIONS AND THE LIFE-TIME OF WATER MOLECULES IN THE FIRST COORDINATION SPHERE

Contents

UNIVERSITY OF CALIFORNIA

ABSTRACT

An investigation was made of the temperature and frequency dependence of T_2 for O^{17} in aqueous solutions containing Mn^{+2}, Fe^{+2}, Co^{+2}, Ni^{+2}, and Cu^{+2}. This represented an extension of the studies previously performed in this laboratory on these ions. Virtually all of the temperature effects predicted by the modified Bloch equations for a two species system were verified experimentally. Rates of exchange of water molecules between the bulk of the solution and the first coordination sphere of the paramagnetic cations were determined for all the ions studied. Activation energies for exchange were measured and electronic T_1's and coupling constants were determined in some cases. Evidence was found for a tetrahedral $Co^{+2}(H_2O)_4$ species in aqueous solutions near 100°C. The data for cupric ion were interpreted in terms of six coordinated water molecules in a distorted octahedron, with a ratio of ca. 10^5 existing for the axial water exchange rate over that of the equatorial waters. The rates of exchange were compared with other physical measurements and the nature of the bonding was considered.

The results of the O^{17} NMR studies were compared with the results of proton NMR studies of the same systems in order to derive additional information.

I. INTRODUCTION AND THEORY

The effect of paramagnetic cations on the transverse relaxation time of O^{17} in nuclear magnetic resonance studies of natural water has been reported previously.[1] More recently, with a water sample which was enriched to 0.7% in O^{17} and with improved experimental techniques, the effect was measured with a much higher degree of accuracy.[2] Lower limits were obtained for the first order rate constants which govern the water exchange process between the bulk of the solution and the first coordination sphere of the cations by means of the relationships established by McConnell and Berger.[1,3] Only limits could be set because it was not known whether the over-all relaxation was controlled by the slowness of the chemical exchange in and out of the first coordination sphere or by the slowness of the O^{17} relaxation process in the first coordination sphere. Bernheim, et al.,[4] have shown that the process governing relaxation can be established in certain cases from the temperature dependence of the overall relaxation.

In the present study the temperature dependence was used to yield rate constants and various parameters controlling the relaxation. A detailed analysis of this temperature function can be derived from the Bloch equations. McConnell[5] has modified the Bloch equations to include the possibility of chemical exchange. In the present work these equations have been applied to the limiting conditions present in a dilute aqueous solution containing paramagnetic ions.

In order to handle the most complex case encountered here, we will treat the three component system. The solution contains the nucleus being observed in three different environments, a,b, and c, with the a

species being much more abundant than b or c. (In the present case of O^{17} a will be the bulk water and b and c will be waters in two different environments in the first coordination sphere of paramagnetic metal ions.) Only slow passage conditions will be considered and the power level is taken to be below saturation so that $M_z^a = M_0^a$, etc., i.e., the z component of magnetization of each species is essentially uninfluenced by the H_0 field. Chemical exchange of the nucleus is permitted between all three species. The appropriate Bloch equations for the steady state, by an obvious extension of McConnell's treatment to three species, are:

$$\begin{aligned} -AG_a + G_b/\tau_{ba} + G_c/\tau_{ca} &= i\,\omega_1\, M_0^a \\ G_a/\tau_{ab} - BG_b + G_c/\tau_{cb} &= i\,\omega_1\, M_0^b \\ G_a/\tau_{ac} + G_b/\tau_{bc} - C\,G_c &= i\,\omega_1\, M_0^c \end{aligned} \qquad (1)$$

where τ_{ab} is the lifetime for the exchange of the nucleus from the a to the b environment, G_a ($= u_a + i\,v_a$) is the complex sum of the in and out of phase field components in the plane perpendicular to H_0, and

$$A = 1/T_{2a} + 1/\tau_{ab} + 1/\tau_{ac} - i\Delta\omega_a \qquad (2)$$

In the last expression T_{2a} is the transverse relaxation time in the a environment and $\Delta\omega_a$ is the difference between the resonance frequency for a and the actual frequency. Solving the three simultaneous equations for G_a yields:

$$G_a = \frac{i\omega_1 \left\{ M_0^a\left(BC - \frac{1}{\tau_{bc}\tau_{cb}}\right) + M_0^b\left(\frac{1}{\tau_{bc}\tau_{ca}} + \frac{C}{\tau_{ba}}\right) + M_0^c\left(\frac{1}{\tau_{ba}\tau_{cb}} + \frac{B}{\tau_{ca}}\right) \right\}}{-ABC + \frac{1}{\tau_{ba}\tau_{cb}\tau_{ac}} + \frac{1}{\tau_{ab}\tau_{bc}\tau_{ca}} + \frac{A}{\tau_{bc}\tau_{cb}} + \frac{B}{\tau_{ac}\tau_{ca}} + \frac{C}{\tau_{ab}\tau_{ba}}} \qquad (3)$$

From the concentration conditions that [a] >> [b] or [c] it follows that $M_0^a >> M_0^b$ or M_0^c and $1/\tau_{ab} \ll 1/\tau_{ba}$, $1/\tau_{ac} \ll 1/\tau_{ca}$. From these inequalities and the relationship $\tau_{ab}\tau_{bc}\tau_{ca} = \tau_{ba}\tau_{cb}\tau_{ac}$ there results as a good approximation:

$$G_a = \frac{i\omega_1 M_0^a (BC - \frac{1}{\tau_{bc}\tau_{cb}})}{-ABC + \frac{2}{\tau_{ab}\tau_{bc}\tau_{ca}} + \frac{A}{\tau_{bc}\tau_{cb}} + \frac{B}{\tau_{ac}\tau_{ca}} + \frac{C}{\tau_{ab}\tau_{ba}}} \qquad (4)$$

In these experiments the part of the signal being observed is that near the pure a resonance. It can be shown by a detailed analysis of terms that the total signal $G(= G_a + G_b + G_c)$ is given to a very good approximation by G_a in this region of the spectrum and for the concentration conditions specified.[6] Writing G in the form resembling that for pure a gives:

$$G = \frac{-i\omega_1 M_0^a}{A - [\frac{2}{\tau_{ab}\tau_{bc}\tau_{ca}} + \frac{B}{\tau_{ac}\tau_{ca}} + \frac{C}{\tau_{ab}\tau_{ba}}] \times \frac{1}{BC - 1/\tau_{bc}\tau_{cb}}} \qquad (5)$$

For the special case that only a - b and a - c exchange are permitted, all terms containing τ_{bc} and τ_{cb} disappear. Clearing the denominator of imaginary terms yields for v, the out of phase component of G:

$$v = \frac{-\omega_1 M_0^a \left[1/T_{2a} + \sum_{j=b}^{c} 1/\tau_{aj} \times \frac{1/T_{2j}^2 + 1/(T_{2j}\tau_{ja}) + \Delta\omega_j^2}{(1/T_{2j} + 1/\tau_{ja})^2 + \Delta\omega_j^2} \right]}{\left[1/T_{2a} + \sum_{j=b}^{c} 1/\tau_{aj} \times \frac{1/T_{2j}^2 + 1/(T_{2j}\tau_{ja}) + \Delta\omega_j^2}{(1/T_{2j} + 1/\tau_{ja})^2 + \Delta\omega_j^2} \right] + \left[\Delta\omega_a + \sum_{j=b}^{c} \frac{\Delta\omega_j}{\tau_{aj}\tau_{ja}(1/T_{2j} + 1/\tau_{ja})^2 + \Delta\omega_j^2} \right]^2} \qquad (6)$$

The first term in brackets in the denominator and the part of the numerator in brackets are essentially frequency independent in the region of interest: either $\Delta\omega_j$ is large and varies little on a percentage basis over the frequency range of interest (the present case) or is so small that its contribution is negligible. Then v will have its maximum value at the frequency where the second term in the denominator equals zero and the half-width at half-height is given to a good approximation by the first brackets in the denominator. The experimental half-width at half-height will be given by the symbol $1/T_2$:

$$1/T_2 = 1/T_{2a} + \sum_{j=b}^{c} 1/\tau_{aj} \; X \; \frac{1/T_{2j}^2 + 1/(T_{2j}\tau_{ja}) + \Delta\omega_j^2}{(1/T_{2j} + 1/\tau_{ja})^2 + \Delta\omega_j^2} \tag{7}$$

The value of $\Delta\omega_a$, i.e., the resonance frequency minus that of pure a is given to a good approximation by:

$$\Delta\omega_a = - \sum_{j=b}^{c} \frac{\Delta\omega_j}{\tau_{aj}\tau_{ja}[(1/T_{2j} + 1/\tau_{ja})^2 + \Delta\omega_j^2]} \tag{8}$$

It is shown in Appendix B that for systems with more than two minor species (exchanging only with the major species) the above equations apply with the summations extended over these species. Equation 7 shows that the experimental quantity, $1/T_2 - 1/T_{2a}$, should contain all relaxation effects arising from the presence of the paramagnetic ions. This quantity will hereafter be referred to as $1/T_{2p}$.

For most of the systems studied the two component case suffices for the interpretation of the experimental data. For solutions containing water and one type of paramagnetic ion Equation 7 gives the following result:

$$1/T_{2\underline{p}} = 1/\tau_{H_2O}\left[\frac{1/T_{2M}^2 + 1/(T_{2M}\tau_M) + \Delta\omega_M^2}{(1/T_{2M} + 1/\tau_M)^2 + \Delta\omega_M^2}\right] \qquad (9)$$

where $\tau_{\underline{ab}}$ and $\tau_{\underline{ba}}$ have been abbreviated to τ_{H_2O} and τ_M.

An analysis of this equation reveals two relaxation mechanisms: one involving T_{2M} which has been considered in detail by Bloembergen, et al.,[7] and Solomon[8,9] and the other involving $\Delta\omega_M$ which has been discussed by McConnell and Berger.[3] The latter -- the $\Delta\omega$ mechanism -- can be of importance if the magnetic environment of the coordinated waters differs by a sufficiently large factor from that of the bulk waters, in which case relaxation can occur through the large change in the precessional frequency of the nucleus in the coordinated state.

The temperature effects predicted by Equation 9 were investigated by a consideration of the following limiting cases:

$$\Delta\omega_M^2 \gg 1/T_{2M}^2,\ 1/\tau_M^2;\ 1/T_{2\underline{p}} = P_M/\tau_M = 1/\tau_{H_2O} \qquad (10A)$$

Relaxation occurs through a change in the precessional frequency and is rapid; $1/T_{2\underline{p}}$ is controlled by the rate of chemical exchange. P_M is given closely by $n[M]/55.5$ where n is the number of coordinated waters per ion and [M] is the molar concentration of the paramagnetic ion.

$$1/\tau_M^2 \gg \Delta\omega_M^2 \gg 1/(T_{2M}\tau_M)\ ;\ 1/T_{2\underline{p}} = P_M\tau_M\Delta\omega_M^2 \qquad (10B)$$

Chemical exchange is rapid; $1/T_{2\underline{p}}$ is controlled by the rate of relaxation through the change in the precessional frequency.

$$1/T_{2M}^2 \gg \Delta\omega_M^2,\ 1/\tau_M^2\ ;\ 1/T_{2\underline{p}} = P_M/\tau_M = 1/\tau_{H_2O} \qquad (10C)$$

Relaxation by T_{2M} is fast; $1/T_{2p}$ is controlled by the rate of chemical exchange.

$$1/(T_{2M}\tau_M) \gg 1/T_{2M}^2,\ \Delta\omega_M^2\ ;\ 1/T_{2p} = P_M/T_{2M} \qquad (10D)$$

Chemical exchange is rapid; $1/T_{2p}$ is controlled by the T_{2M} relaxation process.

The variation of τ_M with temperature is given by:
$\tau_M = (kT/h)^{-1} \exp.\ (\Delta H^{\ddagger}/RT - \Delta S^{\ddagger}/R)$ where $\Delta H^{\ddagger}$ and $\Delta S^{\ddagger}$ are the enthalpy and entropy of activation for the first order reaction of exchange of water from a cation. The temperature dependence of $\Delta\omega_M$ and its relationship to the scalar coupling constant is given by the equation of Bloembergen:[10]

$$\frac{\Delta\omega}{\omega} = \frac{4I(I+1)\ S(S+1)\gamma_e A}{9\ kT\gamma_N} \qquad (11)$$

where I and S are the spins of the nucleus and paramagnetic ion, γ_N and γ_e are the corresponding gyromagnetic ratios, and A/h is the scalar coupling constant. $\Delta\omega_M$ is proportional to T^{-1}. The temperature dependence of T_{2M} will be discussed in the consideration of the experimental results for each ion to which it applies; it is expected to be small or positive.

II. EXPERIMENTAL

The O^{17} resonance signals were recorded with a Varian Associates Model V-4200 wide-line spectrometer operated at 5.43 and 2.00 mc. The sideband technique used previously[2] in these studies was employed. The only significant change was the use of a 15 second time constant in the integrating filter and a correspondingly slow sweep rate of ca. 0.13 gauss per minute. The solutions studied were 2 ml. in volume and were made from enriched water of 1.2% O^{17} and ca. 25% deuterium obtained from the Weizmann Institute of Science. All solutions were 0.1 M. in $HClO_4$.

Temperature studies were made using the sample holder shown in Figure 1. Heated air was passed through the coil in the high temperature work and cooled dry nitrogen was used to maintain low temperatures. The temperature range covered was ca. $0^{\circ}C$ to $100^{\circ}C$.

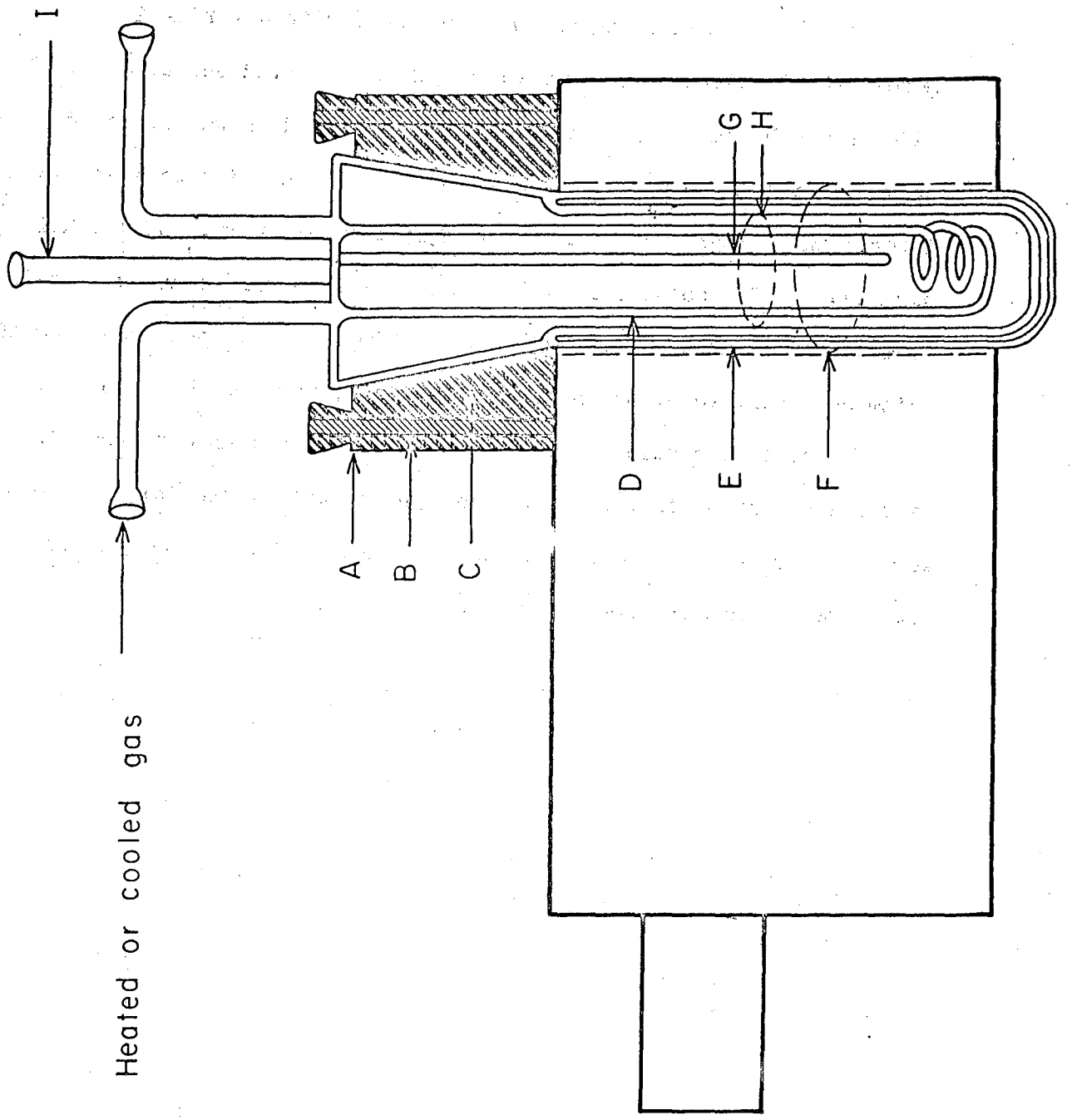

Fig. 1 - Cross section of the all-glass sample holder employed in the temperature studies, shown bolted into the NMR probe. Lettered parts are as follows: (A) Brass block; (B) Brass bolt, welded to probe; (C) Rubber Gasket; (D) Glass coil, 2 mm o.d.; (E) Nonsilvered Dewar; (F) Receiver coil; (G) Thermocouple well; (H) Solution surface; (I) Orifice for filling and evacuating.

MU-25656

III. RESULTS AND DISCUSSION

Since the interpretation of results varies greatly between the different ions studied, each ion is considered separately.

A. Manganous Ion

Bernheim, et al.[4] found that two mechanisms were of importance in the relaxation of protons in aqueous solutions of paramagnetic ions. These are the dipole-dipole[7,8] interaction and the scalar coupling mechanism.[9] The presence of the dipole mechanism was indicated through the effect of the paramagnetic ion on the experimental T_1's since this mechanism produced a nearly equal effect on both T_1 and T_2 under the conditions they employed.

Figure 2 shows the temperature variation of T_2 and T_1 of O^{17} for a 1.82×10^{-4} M solution of $MnSO_4$. Also displayed is the temperature dependence of T_1 and T_2 of the enriched water. The line for T_1 of the manganous solution is shifted from that for water in the direction opposite to that expected for any contribution from the manganous ion. The rather large difference in the positions of the two T_1 lines with respect to each other is believed to arise from experimental uncertainty which is inherently high in the saturation method for the determination of T_1's. Within the accuracy of the T_1 determinations, the manganous ions produce no effect on T_1 and therefore the dipole-dipole relaxation mechanism was considered to produce only a negligible effect. This was found to be true for cupric ion also, and Dr. E. Genser[11] of this laboratory has indications of the same result for ferric ion in 1 M nitric acid. Values of T_1 were not measured for Fe^{++}, Co^{++} and Ni^{++}. The T_2 data for these ions give no indication of a dipole-dipole contribution, although a small one could be present.

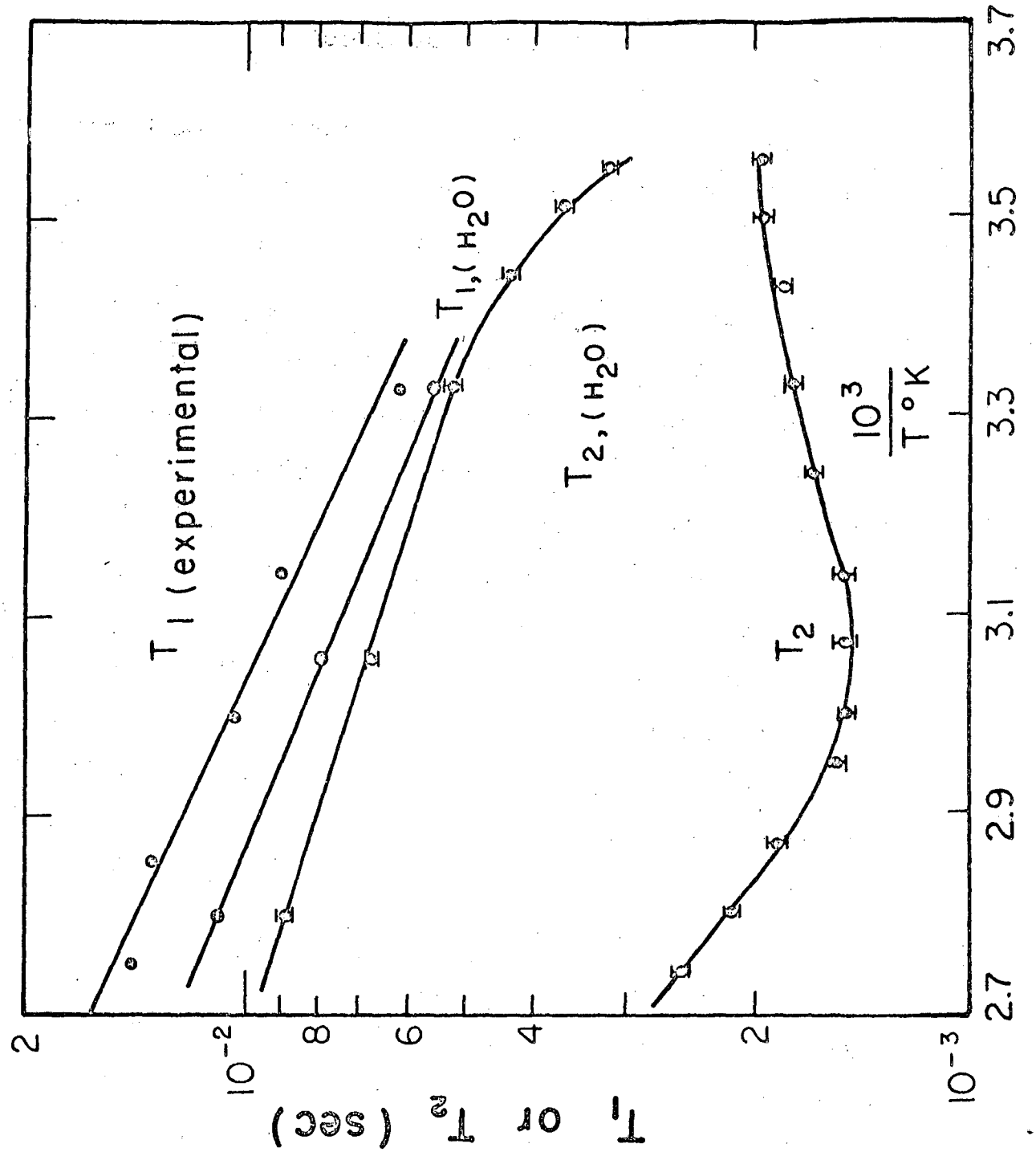

Fig. 2 - Dependence on reciprocal of temperature of log T_2 for a 1.82×10^{-4} M solution of $MnSO_4$. Also shown are the temperature dependences of log $T_{1\,exp}$ and log T_{2H_2O} and log T_{1H_2O}.

MU-25653

Figure 3 shows the temperature dependence of T_{2p} and it reveals that the dependence at low temperature corresponds to that of a chemical reaction, which must correspond to region 10A or 10C. The approximate value of τ_{Mn} obtained from the data at low temperature eliminates the $\Delta\omega$ mechanism from consideration in this case: an impossibly high value of the coupling constant would be necessary to account for the data. The low temperature region is then 10C and the high temperature results lie in region 10D.

In order to subject the data of Figure 3 to a curve fitting process the temperature dependence of T_{2Mn} had to be known. From Bernheim, et al.,[4] T_{2Mn} is expected to be given by:

$$1/T_{2Mn} = 4/9I(I + 1)S(S + 1)\frac{A^2}{\gamma_n^2}\tau_e = C\tau_e,$$

in the frequency region of interest. The value of the correlation time τ_e is given by $1/\tau_e = 1/T_{1e} + 1/\tau_{Mn}$, where T_{1e} is the electronic T_1. At high temperatures T_{2Mn} will be controlled by the interruption arising from chemical exchange, while at lower temperatures the electronic interruption will dominate. Thus, at high temperatures one expects a limiting slope equal in magnitude but opposite in sign to that observed for region 10C at low temperature, as has been drawn for the high and low temperature limiting slopes in Fig. 3. In between the two extremes an appreciable contribution from the term controlled by electronic interruption can occur as is shown in the nearly horizontal line. Bloembergen and Morgan's[12] Equations 22 and 24 were used to calculate the temperature dependence of T_{1e}, taking V_v = 1.00 kcal from the data of Codrington and Bloembergen.[13]

The curve which passes through the experimental points of Figure

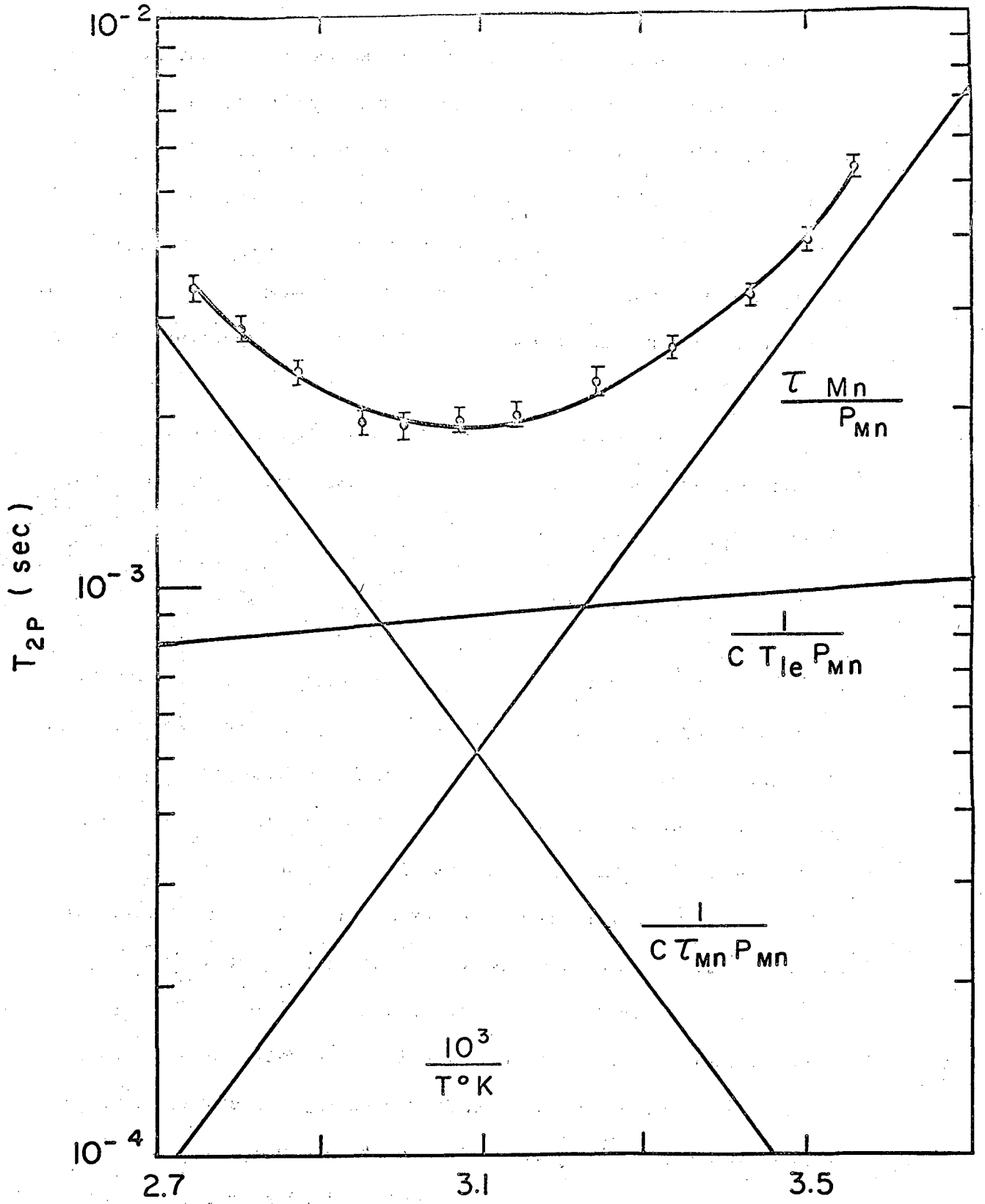

Fig. 3 - Temperature dependence of log T_{2p} for a 1.82×10^{-4} M $MnSO_4$ solution with the lines resulting from the curve-fitting.

3 was calculated as the sum of the three lines shown in the Figure according to Equation 9, which reduces in this case to

$$1/T_{2p} = \frac{\frac{1}{\tau_{H_2O} T_{2Mn}}}{1/T_{2Mn} + 1/\tau_{Mn}} = \frac{P_{Mn}}{\tau_{Mn} + T_{2Mn}} = \frac{P_{Mn}}{\tau_{Mn} + \frac{1}{C}(1/T_{1e} + 1/\tau_{Mn})} \qquad (12)$$

where C is a temperature independent constant. The three lines shown represent the best fit to the data, if the electronic T_1 is maintained near the experimentally[12,13,14,15] observed value of ca. 3×10^{-9} sec.

Table I gives the values of some parameters determined through the curve-fitting process. A comparison is given between these values and those obtained in the proton NMR work.[4,12] The similarity leaves no doubt of the correctness of the earlier suggestion of Pearson et al.,[16] that the proton exchange occurs by the exchange of whole water molecules under the conditions used by Bernheim et al.[4]

The larger value of the coupling constant for O^{17}, as compared to that of the proton, results in an enhancement of the scalar coupling relaxation and explains why the dipole-dipole mechanism was not observed.

No chemical shift was detected in solutions of Mn^{+2}. This is consistent with the A/h value listed in Table I. A calculation showed that the line broadening is much larger than the shift and thus the shift is obscured.

B. Cupric Ion

Figure 4 shows the variation of T_{2p} with temperature for a 1.00×10^{-3} M solution of $Cu(NO_3)_2$. Excluding for a moment the high temperature bend, the data show a region of rather high negative slope where the rate is presumably controlled by the slowness of relaxation. This corresponds to a region 10B or 10D and indicates that very low

TABLE I

Parameters from Figure 3 for Exchange of O^{17} and Protons Between the First Coordination Sphere of Mn^{+2} and Bulk Water

Quantity	Oxygen	Proton (Ref. 4)	Proton (Ref. 12)
$\Delta H^{\ddagger}$ (kcal)	8.1	7.8	7.5
k_1 (sec^{-1} at 298°K)	3.1×10^7	3.6×10^7	4.0×10^7
T_{1e} (sec at 298°K and low field)	3.8×10^{-9}	3.0×10^{-9}	3.5×10^{-9}
A/h (cps)	2.7×10^6	$\sim 1 \times 10^6$	1.0×10^6
$\Delta S^{\ddagger}$ (eu)	2.9	2.2	1.3

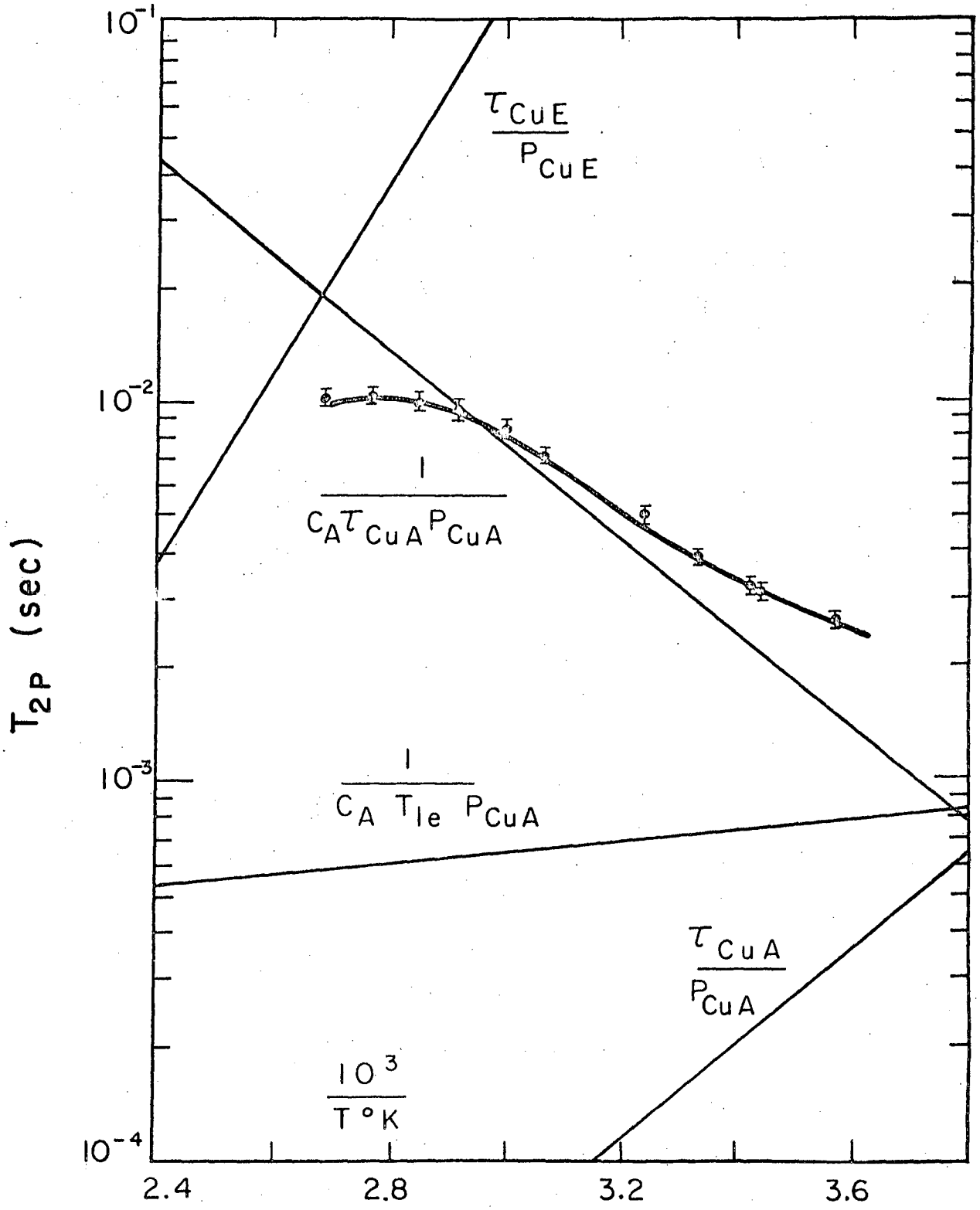

Fig. 4 - Temperature dependence of log T_{2p} for a 1.00×10^{-3} M $Cu(NO_3)_2$ solution with the lines resulting from the curve fitting.

MU-25644

temperatures would have to be attained in order to observe the region where the relaxation is determined by the rate of the water exchange process. From the value of T_{2p} at the lowest temperature shown in Figure 4 an upper limit was calculated for τ_{Cu}. This value is ca. 1×10^{-8} sec., and again the $\Delta\omega$ mechanism may be ignored on the basis of an impossibly high coupling constant. As was the case with the Mn^{+2} solutions, lines corresponding to regions 10C and 10D could be added to give a curve through the experimental data at temperatures less than ca. 80°C.

The bendover at high temperatures is reversible with respect to temperature. The data clearly show the threshold of another region where the relaxation is occurring by a new path involving cupric ion. The possibility of dipole-dipole coupling must be discarded for two reasons: it should be much smaller than scalar coupling and T_{2p} should show a more negative dependence on the reciprocal of temperature than the data appear to give at the highest temperature. Measurements of T_1 were carried only to 80°C and therefore gave essentially no information about the bendover region. If scalar coupling is still involved, there must be more than one kind of oxygen associated with the copper.

The Cu^{+2} ion in crystals has long been known to coordinate with four water molecules in a quite stable square-planar arrangement. For example in $CuSO_4 \cdot 5H_2O$ the Cu^{+2} is octahedrally coordinated with four waters in a plane having their oxygens 1.95 to 2.05 Å from the Cu^{+2} and two sulfate oxygens at the poles having their oxygens 2.32 to 2.45 Å from the Cu^{+2}.[17] It is also thought that in aqueous solution the Cu^{+2} ion coordinates with six water molecules to form such a distorted octahedron. This hypothesis can be used to explain the NMR data.

The results of the low temperature curve-fitting of Figure 4 show conclusively the presence of a quite labile form of coordinated water, presumably the axially coordinated form. The high temperature effect then likely arises from exchange of waters from the equatorial positions.

There are two plausible mechanisms for equatorial water exchange:

(a) Direct exchange with the bulk waters at the equatorial positions.

(b) An inversion process in the $Cu^{+2}(H_2O)_6$ ion in which the axial positions become equatorial and two of the equatorial positions become axial. This process may then be followed by the rapid water exchange from the axial positions.

The data are such that no choice is possible between these two alternative mechanisms.

A large range of values for necessary parameters can be found which results in lines which add to reproduce the data of Figure 4. In order to constrict the range of solutions the following considerations are made.

The entropies of activation of the water exchange processes for all the ions studied had small values. Therefore it was expected that the loosely bound waters in the axial positions of the hydrated cupric ion would go through an entropy of activation of ca. zero.

Bloembergen and Morgan[12] and Kivelson[18] have shown that the functional relationship existing between the electronic T_1 and temperature is closely linked with the motion of the bulk water molecules in the neighborhood of the paramagnetic ions. The activation energy governing the T_1 relaxation may be considered as a first approximation to be independent of the nature of the paramagnetic ion. Since the experimental temperature dependence of the electronic T_1 of Mn^{+2} has been

shown to be very small, the approximation given above probably cannot produce a sizeable error. Consequently the same slope was used here as was used in the Mn^{+2} case.

Hayes[19] has partially resolved the ESR spectrum of cupric ion in aqueous solutions near 0°C. The value obtained for the electronic T_2 is ca. 5×10^{-9} sec. Kivelson[18] has shown that T_1 may be larger than T_2 for cupric ion because of the anisotropic $\underline{g}$ factor. The curve-fitting process was then required to yield a value of T_{1e} which was $> 5 \times 10^{-9}$ sec.

Coupling constants have also been obtained for all ions studied here and they range from $1\text{-}4 \times 10^{6}$ cps. The loosely bound axial water molecules on a cupric ion certainly cannot possess a coupling constant which is greatly above this range.

The mathematical problem of curve-fitting was handled through a consideration of Equation 7; which becomes

$$1/T_{2\underline{p}} = P_{CuA}/\tau_{CuA}\left[\frac{1/T_{2CuA}^{2} + 1/(T_{2CuA}\tau_{CuA}) + \Delta\omega_{CuA}^{2}}{(1/T_{2CuA} + 1/\tau_{CuA})^{2} + \Delta\omega_{CuA}^{2}}\right] + P_{CuE}/\tau_{CuE}\left[\frac{1/T_{2CuE}^{2} + 1/(T_{2CuE}\tau_{CuE}) + \Delta\omega_{CuE}^{2}}{(1/T_{2CuE} + 1/\tau_{CuE})^{2} + \Delta\omega_{CuE}^{2}}\right] \quad (13)$$

where $P_{CuE} = 4[Cu]/55.5$, $P_{CuA} = 2[Cu]/55.5$, and A and E refer to axial and equatorial, respectively. This equation would apply to the case where the equatorial water exchange occurs directly with the bulk water.

A consideration of the conditions shown by the temperature effects of Figure 4 reduces Equation 13 for the relaxation time to the following relation:

$$1/T_{2\underline{p}} = \underbrace{\frac{P_{CuA}}{\tau_{CuA} + T_{2CuA}}}_{(a)} + \underbrace{\frac{P_{CuE}}{\tau_{CuE}}}_{(b)} \quad (14)$$

The lines in Fig. 4 which represent the terms (a) and (b) of Equation 14 do not combine by simple addition to reproduce the experimental results. Instead the two lines which make up (a) add to give that part of the data which excludes the high temperature bend and then $1/(a) + 1/(b)$ gives the reciprocal of the bendover region of Fig. 4. The lower temperature points were subjected to curve-fitting under the restrictions previously outlined. The line corresponding to (b) was then obtained as a remainder. Table II gives the values of some quantities calculated from the lines shown in Fig. 4.

For the chemical exchange process to control $T_{2\underline{p}}$ at high temperature, the numerator and denominator of the brackets of Equation 9 must be very nearly equal. This relationship obtains if:

$$1/(T_{2CuE}\tau_{CuE}) + 1/\tau_{CuE}^2 \ll 1/T_{2CuE}^2 + \Delta\omega_{CuE}^2 \qquad (15)$$

At 97°C, this inequality becomes:

$$2.2(A/h)^2 + 4.0 \times 10^{11} \ll 1.2 \times 10^{-11}(A/h)^4 + 4.2 \times 10^{-3}(A/h)^2 \qquad (16)$$

It is seen that $1/(T_{2CuE}\tau_{CuE}) \gg \Delta\omega_{CuE}^2$ and the $\Delta\omega$ mechanism may be discarded in the interpretation of the high temperature relaxation. The lower limit of A/h obtained from Equation 16 is given in Table II.

The possibility is now considered that exchange of equatorial waters occurs through inversion of the distorted octahedron of waters, coupled with rapid exchange of axial waters. Starting with Equation 5 and imposing the additional restriction that $\underline{a}$-$\underline{c}$ exchange is negligible yields:

$$G = \frac{-i\omega_1 M_0^{\underline{a}}}{A - \dfrac{1}{\tau_{\underline{ab}}\tau_{\underline{ba}}\left(B - \dfrac{1}{C\tau_{\underline{bc}}\tau_{\underline{cb}}}\right)}}$$

Solving this equation as before for the half-width at half-height gives as a good approximation.

TABLE II

Values Calculated from Fig. 4 for a 1.00×10^{-3} M Solution of Cu^{+2}

Quantity	Equatorial	Axial
$\Delta H^{\ddagger}$ (kcal)	11	5
k_1 (sec^{-1} at 298°K)	1.0×10^{4}	2×10^{8}
T_{1e} (sec at 298°K)	- - - - -	2×10^{-8} [a]
A/h (cps)	$\gg 5.5 \times 10^{5}$	4×10^{6}
$\Delta S^{\ddagger}$ (eu)	-4	-4

[a]The value is of course independent of the position of coordination; but the calculation was made from data corresponding to axial water exchange.

$$\frac{1}{T_2} = \frac{1}{T_{2a}} + \frac{1}{\tau_{ab}} - \frac{1}{\tau_{ab}\tau_{ba}} \times \frac{\frac{1}{T_{2b}} + \frac{1}{\tau_{ba}} + \frac{1}{\tau_{bc}} \times \frac{\frac{1}{T_{2c}^2} + \frac{1}{T_{2c}\tau_{cb}} + \Delta\omega_c^2}{(\frac{1}{T_{2c}} + \frac{1}{\tau_{cb}})^2 + \Delta\omega_c^2}}{\left\{\frac{1}{T_{2b}} + \frac{1}{\tau_{ba}} + \frac{1}{\tau_{bc}} \times \frac{\frac{1}{T_{2c}^2} + \frac{1}{T_{2c}\tau_{cb}} + \Delta\omega_c^2}{(\frac{1}{T_{2c}} + \frac{1}{\tau_{cb}})^2 + \Delta\omega_c^2}\right\}^2 + \left\{\Delta\omega_b + \frac{\Delta\omega_c}{\tau_{bc}\tau_{cb}\left[\left(\frac{1}{T_{2c}} + \frac{1}{\tau_{cb}}\right)^2 + \Delta\omega_c^2\right]}\right\}^2} \qquad (17)$$

Since the experimental data indicate that $\Delta\omega$ terms are unimportant, one has for the case of interest

$$\frac{1}{T_2} = \frac{1}{T_{2a}} + \frac{1}{\tau_{ab}} \times \frac{\frac{1}{T_{2b}} + \frac{1}{T_{2c}\tau_{bc}(\frac{1}{T_{2c}} + \frac{1}{\tau_{cb}})}}{\frac{1}{T_{2b}} + \frac{1}{\tau_{ba}} + \frac{1}{T_{2c}\tau_{bc}(\frac{1}{T_{2c}} + \frac{1}{\tau_{cb}})}}$$

In the region of the high temperature bend the temperature dependence indicates that $1/\tau_{ba}$ dominates the denominator and $1/T_{2c} \gg 1/\tau_{cb}$; thus

$$\frac{1}{T_2} = \frac{1}{T_{2a}} + P_b(\frac{1}{T_{2b}} + \frac{1}{\tau_{bc}})$$

For the higher temperature region Equation 14 has precisely this same algebraic form, and, therefore, the shape of the temperature dependence curve is not indicative of the mechanism.

The data are such that little in the way of numerical accuracy can be obtained for the quantities which deal with the equatorial water exchange. A much more accurate value of $\Delta H^{\ddagger}$ and of τ_{CuE} could be obtained through determinations of T_{2p} at temperatures in excess of 100°C.

Finally, a calculation of the ratio of chemical shift to line broadening led to a prediction of no detectable chemical shift, which was the experimental result.

C. Nickelous Ion

An extremely large temperature effect was observed for the T_{2p} of Ni^{+2} solutions at 5.43 mc as is shown in Fig. 5. In order that the entire temperature range from 0 to 100°C could be examined, three solutions of concentrations 0.100 M, 3.39×10^{-2}M, and 6.12×10^{-3}M $Ni(NO_3)_2$ were employed. Previous experiments[2] had shown that a linear relationship exists between $1/T_2$ and the concentration of the paramagnetic ion. This was confirmed with the three Ni^{+2} solutions mentioned above and all results of Figs. 5 and 6 were referred to a value for a 0.100 M solution.

The conditions existing in the solution at temperatures in the linear region of Fig. 5 quite clearly are 10A or 10C. The value of τ_{Ni} calculated from the linear region, however, along with the very small electron spin[20] relaxation time thought to exist for Ni^{+2} in aqueous solutions, make 10A more plausible. The high temperature bend is then due to the threshold of region 10B. Table III gives the numerical results of the curve-fitting.

The limit of T_{1e} was assessed from the high temperature data. By a combination of regions 10B and 10D the following region is obtained when the relationship between $\Delta\omega_M^2$ and $1/T_{2M}^2$ is not known:

$$1/\tau_M^2 \gg \Delta\omega_M^2 + 2\,(T_{2M}\tau_M) \; ; \quad 1/T_{2p} = P_M/T_{2M} + P_M\tau_M\Delta\omega_M^2$$

Table III

Values Calculated from Figs. 5 and 6 for Exchange of Water from the First Coordination Sphere of Ni^{+2}

Quantity	Value
$\Delta H^{\ddagger}$ (kcal)	11.6
k_1 (sec^{-1} at 298°K)	2.7×10^{4}
T_{1e} (sec at 298°K)	$\leqslant 1.3 \times 10^{-11}$
A/h (cps)	3.6×10^{6}
$\Delta S^{\ddagger}$ (eu)	0.6

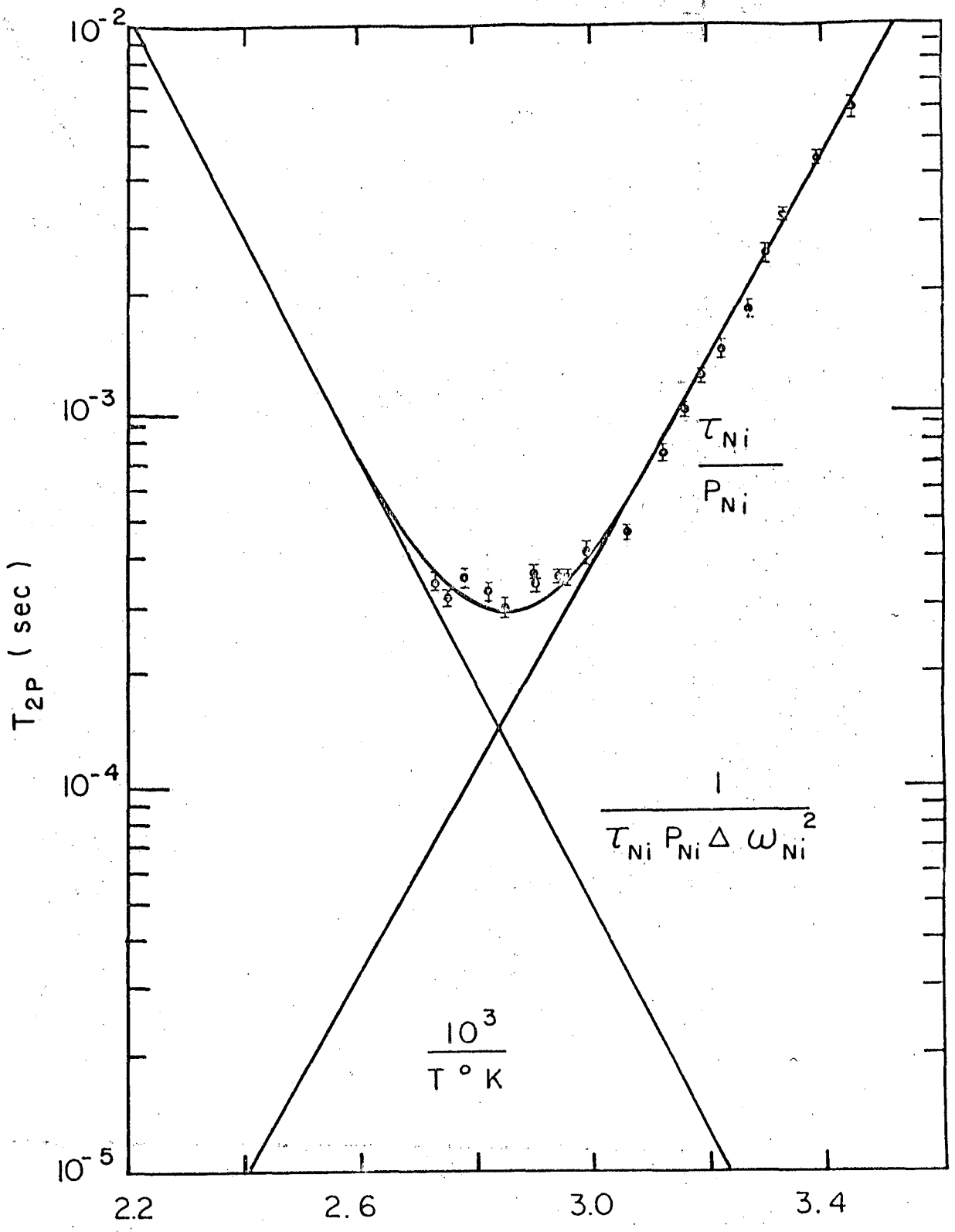

Fig. 5 - Temperature dependence of log T_{2p} for a 0.100 M solution of Ni $(NO_3)_2$ at 5.43 Mc. The lines resulting from the curve-fitting process are also shown. Data from 3.39×10^{-2} and 6.12×10^{-3} M solutions were corrected to 0.100 M.

MU-25654

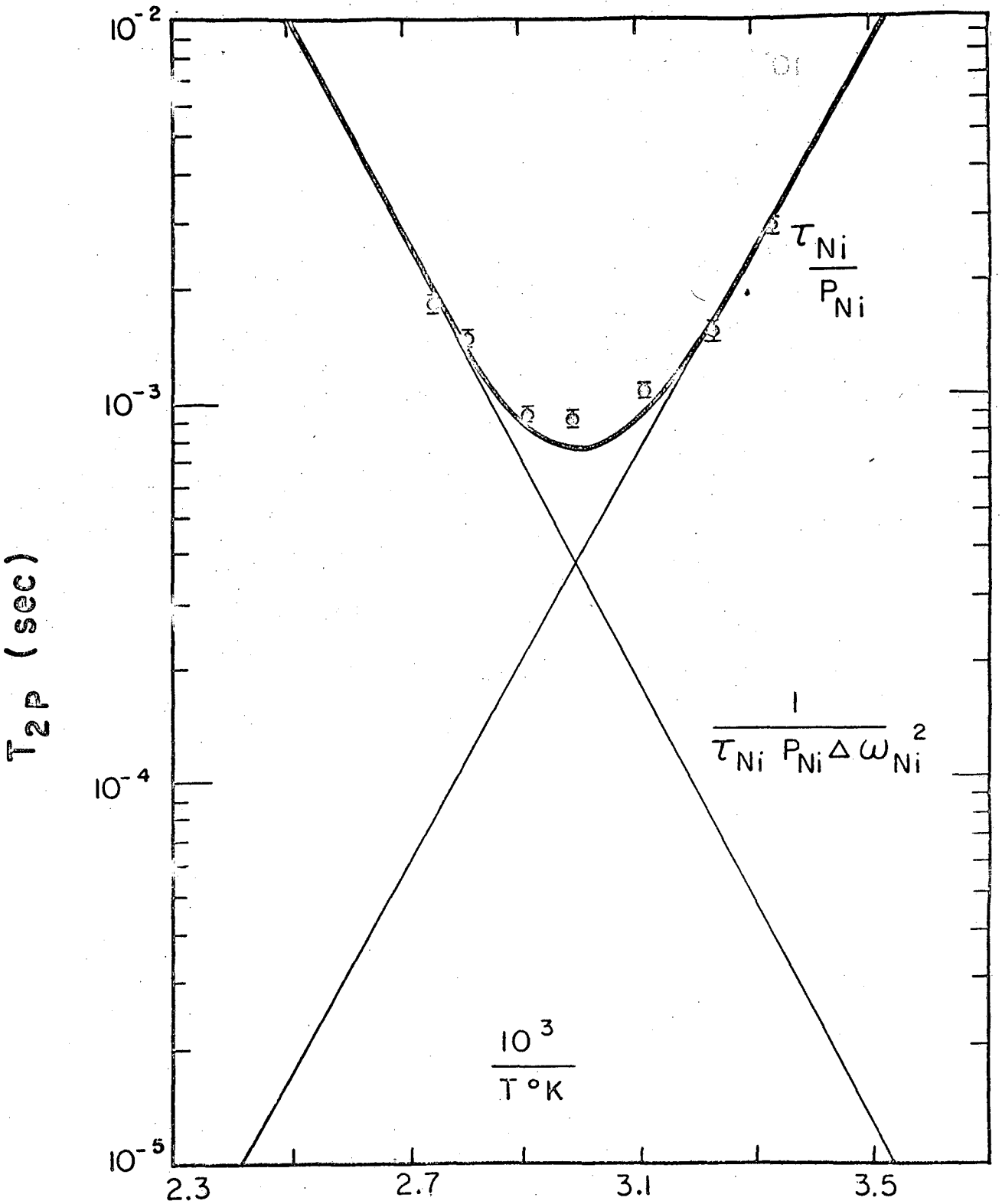

Fig. 6 - Temperature dependence of log T_{2p} of a 0.100 M $Ni(NO_3)_2$ solution. The concentration actually used was 0.200 M but the values were referred to the corresponding value for the more dilute solution for purposes of comparison with Fig. 5. The frequency was 2.00 Mc.

MU-25647

From previous considerations and from the frequency study discussed below, it is known that $P_M \tau_M \Delta \omega_M^2$ is the larger of these two terms. For the purposes of obtaining a limit for T_{2M} these two terms were equated. This method was also used in the determination of the limits of the electron spin relaxation times of Co^{+2} and Fe^{+2}. The resulting limits in all three cases were consistent with estimated limits.[20]

A check on the assumption that the conditions correspond to regions 10A and 10B was provided by the frequency dependence of T_{2p}. Figure 6 shows the temperature variation of T_{2p} of a 0.100 M $Ni(NO_3)_2$ solution at 2.00 mc. The two straight lines correspond to the lines of Fig. 5 with the correction made for the change in frequency according to Equation 11 which predicts a linear dependence of $\Delta\omega$ on frequency The curve which represents the sum of the two lines of Fig. 5 fits the data every bit as well as the lines of Fig. 5 fit the points of Fig. 5. This demonstrates that the $\Delta\omega$ mechanism can produce appreciable relaxation in solutions of paramagnetic ions and also that the value of $\Delta\omega_{Ni}$ is quite accurately known.

The chemical shift is still not observable in Ni^{+2} solutions at 298°K even though the broadening is quite small compared to Mn^{+2} or Cu^{+2} solutions. By an analysis of Equation 8 under the conditions of 10A the shift at 5.43 mc is predicted to be:

$$\Delta\omega_{H_2O} = -P_{Ni}\Delta\omega_{Ni}\left(\frac{1}{\tau_{Ni}^2\Delta\omega_{Ni}^2}\right) \qquad (17)$$

Since $\Delta\omega_{Ni}^2 \gg 1/\tau_{Ni}^2$ at 298°K the shift is only a fraction of its maximum value and is undetectable. Near 100°C, however, the shift is given to a good approximation by:

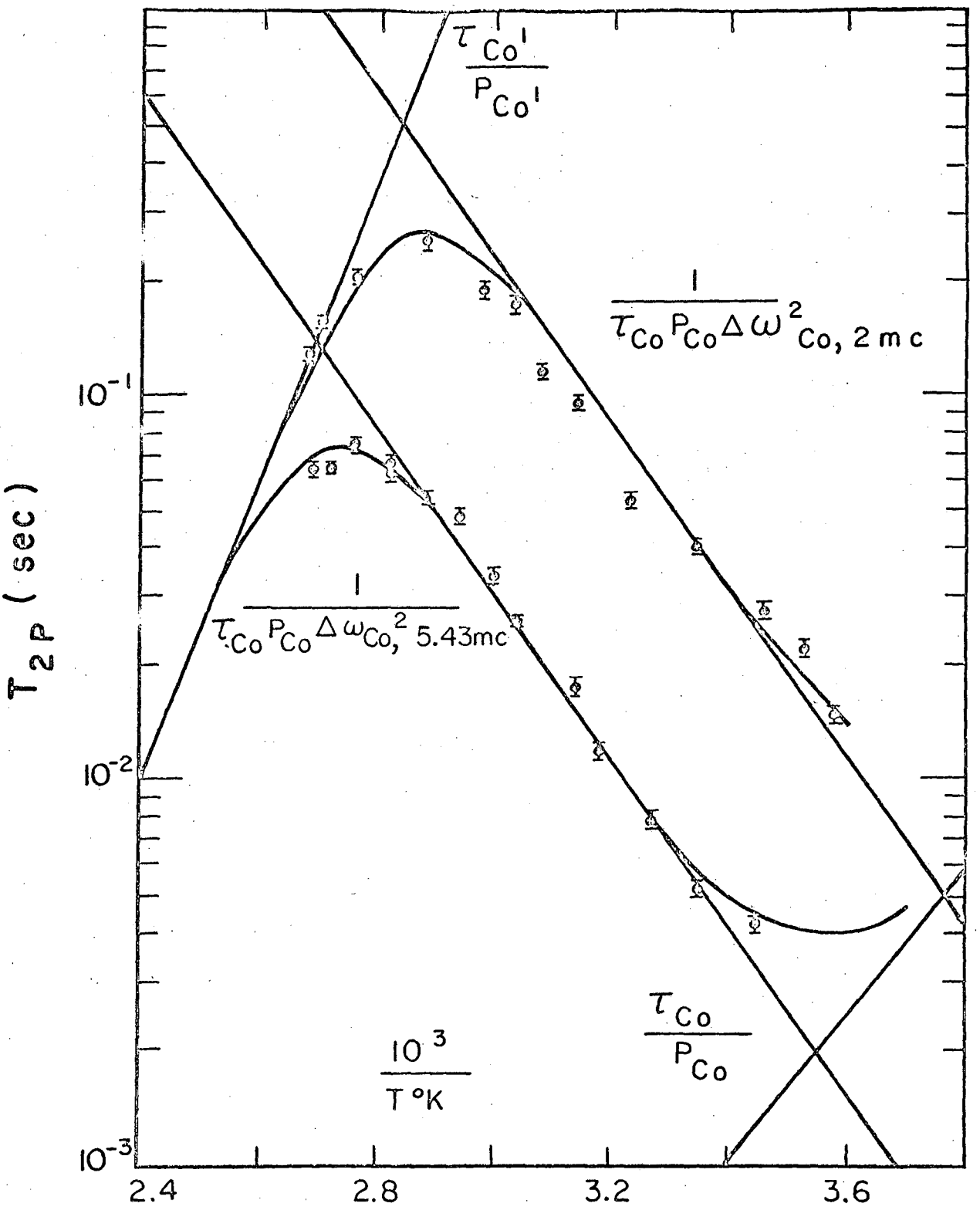

Fig. 7 - Temperature dependence of T_{2p} of $CoSO_4$ and $Co(ClO_4)_2$ solutions at 5.43 mc. and 2.00 mc. The lines resulting from the curve-fitting are also shown. All data are corrected to 1.00×10^{-2} M Co^{+2}.

$$\Delta\omega_{H_2O} = -P_{Ni}\Delta\omega_{Ni}$$

A calculation revealed that a paramagnetic shift should be observed, and a sizeable shift was observed experimentally. The value of the coupling constant calculated from the chemical shift at elevated temperatures was imprecise and consequently is not given.

D. Cobaltous Ion

As with the Ni^{+2} solutions the solutions of Co^{+2} display a marked temperature variation in T_{2p} as shown in Fig. 7. The upper points were obtained at 2.00 mc, and the lower points at 5.43 mc. The solutions used in the work at 5.43 mc were 1.00×10^{-2}, 4.77×10^{-2}, and 0.163 M in $CoSO_4$, and 0.147 M in $Co(ClO_4)_2$. Those used in the 2.00 mc experiments were 7.63×10^{-2} and 0.223 M in $CoSO_4$. The values for all concentrations were referred to the corresponding values for a 1.00×10^{-2} M solution in Fig. 7.

The ratio of the T_{2p}'s for the two frequencies at $300^{\circ}K$. definitely indicates that the linear regions in the intermediate temperature range are 10B. The predicted ratio for 10B is $(5.43/2.00)^2$, or 7.35. This observation is also consistent with the estimated limit[20] for the electronic T_1. The bend at low temperatures is then due to 10A.

The reversible high temperature bend presents more difficulty in interpretation, as did the similar bend in the case of the Cu^{+2} solutions. An examination of Equation 9 shows that such a bendover from the $\Delta\omega$ relaxation controlled region cannot occur through scalar coupling for the two component system (assuming the temperature dependence of T_{1e} to be small or negative). As reasoned for Cu^{+2}, dipole-dipole relaxation should

not be important. Once again the only recourse is the introduction of a new species into consideration.

In spite of the bending regions in Fig. 7 the curve fitting was much easier and more precise, than with the Cu^{+2} data. The curves in Figure 7 were subjected to the fitting process simultaneously with the restriction that the ratio of the T_{2p}'s at 30°C be 7.35. Table IV gives the results of this operation for parameters involving water exchange from the Co^{+2} $(H_2O)_6$ species.

Measurement of the chemical shift provided a confirmation for the assumption of 10B conditions as well as the values of τ_{Co} and A/h. Solutions of Co^{+2} show broader line widths than Ni^{+2} solutions of the same concentration. Equation 8, however, under conditions 10B yields the following relationship for the chemical shift:

$$\Delta\omega_{H_2O} = -P_{Co}\Delta\omega_{Co} \qquad (18)$$

Thus the shift has assumed its maximum value. The measured paramagnetic shift at 1.00×10^{-2} M Co^{+2} and 300°K was 14.0 ppm. Jackson, et al.[21] found a paramagnetic shift of 330 ppm in a 0.2 M Co^{+2} solution at ca. 300°K, which is slightly larger than found here.

A value of the coupling constant was calculated from the Bloembergen equation[10] using the value of 14.0 ppm for the shift. By this calculation A/h was found to be 1.14×10^6 cps. The value of A/h calculated from the chemical shift was then used to calculate k_1 at 298°K. Figure 7 contains the chemical exchange controlled line corresponding to this value of k_1.

The relaxation process which enters at high temperatures has a high activation energy and certainly corresponds to regions 10A or 10C. Equation 7 adapted to give the high temperature bend is:

Table IV

Values Calculated from Fig. 7 for Exchange of Water from the First Coordination Sphere of Co^{+2}

Quantity	Value
$\Delta H^{\ddagger}$ (kcal)	8.0
k_1 (sec^{-1} at 298°K)	1.13×10^{6}
T_{1e} (sec at 298°K)	$< 5 \times 10^{-12}$
A/h (cps)	1.14×10^{6}
$\Delta S^{\ddagger}$ (eu)	-4.1

$$1/T_{2p} = P_{Co}\,[\tau_{Co}\Delta\omega_{Co}^{2}] + P_{Co'}/\tau_{Co'} \qquad (19)$$

where the primes indicate the high temperature species.

The presence of a new species which reveals itself at high temperatures suggested an equilibrium analogous to the $4Cl^{-} + Co^{+2} \rightleftharpoons CoCl_4^{-2}$ system of cobalt chloride complexes. The possibility of an anion effect was discounted through a determination of T_{2p} from 80 to 100°C in solutions of $Co(ClO_4)_2$. No difference was detected from the sulfate results.

The treatment of a possible explanation for the high temperature data of Fig. 7 will be as follows. The data will be discussed in a general manner in order to obtain some characteristics of the new cobalt species and then will be interpreted in terms of the new species being tetrahedral $Co^{+2}(H_2O)_4$ in order to show that this ion yields results which are in agreement with the observations.

Figure 7 shows that at 94.5°C the ratio $(\tau_{Co'}/P_{Co'})/(\tau_{Co}/P_{Co})$ is equal to 5.0×10^3. The large value of this ratio may be due to the small concentration of the new species or to a large difference in the water exchange rates or to a combination of the two.

Assuming the primed cobalt species to be a minor constituent even at the high temperatures, the slope of the $\tau_{Co'}/P_{Co'}$ line yields 17 kcal for $\Delta H = \Delta H^{\ddagger}_{Co'} + \Delta H_{Co\text{-}Co'}$, where the heat of activation refers to the water exchange process for the primed species and $\Delta H_{Co\text{-}Co'}$ is the enthalpy change for the conversion of the Co^{+2} to the primed cobalt species. From the lifetimes the corresponding free energy change $\Delta F = \Delta F^{\ddagger}_{Co'} + \Delta F_{Co\text{-}Co'}$ is found to be 15.2 kcal at 94.5°C. The entropy change $\Delta S = \Delta S^{\ddagger}_{Co'} + \Delta S_{Co\text{-}Co'}$ is then 5 eu. The entropy change can give information about the nature of the exchange process. Compared to $\Delta S^{\ddagger}_{Co}$ the 9 eu more positive value of

ΔS would be consistent qualitatively with a four-coordinated cobaltous ion exchanging water molecules directly. Thus $\Delta S^{\ddagger}_{Co'}$ might be expected to be a small negative quantity as found for $\Delta S^{\ddagger}_{Co}$, but $\Delta S_{Co-Co'}$ should be appreciably positive because of the freeing of two water molecules.[22] Alternatively the four coordinated species might exchange water molecules by conversion to the six coordinated species and vice versa. A fairly positive entropy would be expected, once again, if the activated complex had less than six fold coordination, e.g., five fold. Actually the precision of the present data does not warrant drawing any definite conclusions. Measurements at higher temperatures are underway in this laboratory to fix the high temperature activation energy and entropy more precisely.

Since the octahedrally coordinated cobalt is the only uncomplexed species ever identified in an aqueous solution near room temperature, the concentration of the Co' species at high temperatures is no doubt small. Also the long linear region at the intermediate temperatures indicates that the concentration of the octahedral species is virtually a constant, an observation which reinforces the idea that the new species is present at a relatively low concentration. It is possible, of course, that the $Co^{+2}(H_2O)_6$ ion possesses nonequivalent positions as with $Cu^{+2}(H_2O)_6$. Such a case would explain the high temperature data; however the ratio between the water exchange rates at the two different positions at 94.5°C would have to be $> 1 \times 10^4$, a larger value than exists for $Cu^{+2}(H_2O)_6$ at the same temperature. X-ray crystal studies indicate much less deformation for octahedrally coordinated Co^{+2} salts than for Cu^{+2} salts.

In order to investigate the possible presence of a new species at high temperatures, the visible spectrum of a 0.600 M solution of $CoSO_4$ which

was also 0.1 M in $HClO_4$ was measured as a function of temperature using a Cary Recording Spectrophotometer. The solution was heated and the temperature was maintained at 94.5°C by means of an asbestos board box which contained a sealed 5 mm. cell, a cell holder, a thermocouple, and two 22 mm. quartz windows. Alignment of the windows with the light path was achieved by designing the box so that it fitted exactly on the Cary cell holder plate. Heated air was circulated through the box to maintain the temperature.

Figure 8 shows the spectra at 27°C and 94.5°C. The difference between these spectra indicates the growth of a new peak at ca. 550 mμ. Since the tetrahedral complex was expected[23] to have a smaller crystal field effect than the octahedral complex, the result is consistent qualitatively with the formation of the tetrahedral species. If the tetrahedral aquo complex has similar spectral characteristics to the known tetrahedral halide complexes,[24] it possesses a maximum molar extinction coefficient which is a factor of 10^2 higher than the maximum molar extinction coefficient of the octahedral species. The use of this ratio, along with the spectra of Fig. 8, gives a value of 4×10^2 for the ratio of $P_{Co}/P_{Co'}$. The resulting ratio of $\tau_{Co'}/\tau_{Co}$ would then be 13 at 94.5°C.

If these approximate values of the concentrations and the rates of water exchange are used, the following results may be deduced. The rate $1/\tau_{Co'}$ equals 12 $\Delta\omega_{Co}$ at 2.00 mc. For condition 10A to hold in the high temperature region it is necessary that $1/\tau_{Co'} \ll \Delta\omega_{Co'}$ and therefore $\Delta\omega_{Co'}$ would have to be considerably greater than $\Delta\omega_{Co}$ -- at least 20 fold. There is no guide to the plausibility of such a condition. If instead conditions 10C exist at high temperature, T_{1e} for Co' must be considerably larger than for Co, i.e., $T_{1e} \geqslant 5 \times 10^{-8}$ sec. Again the plausibility of such a condition is not known.

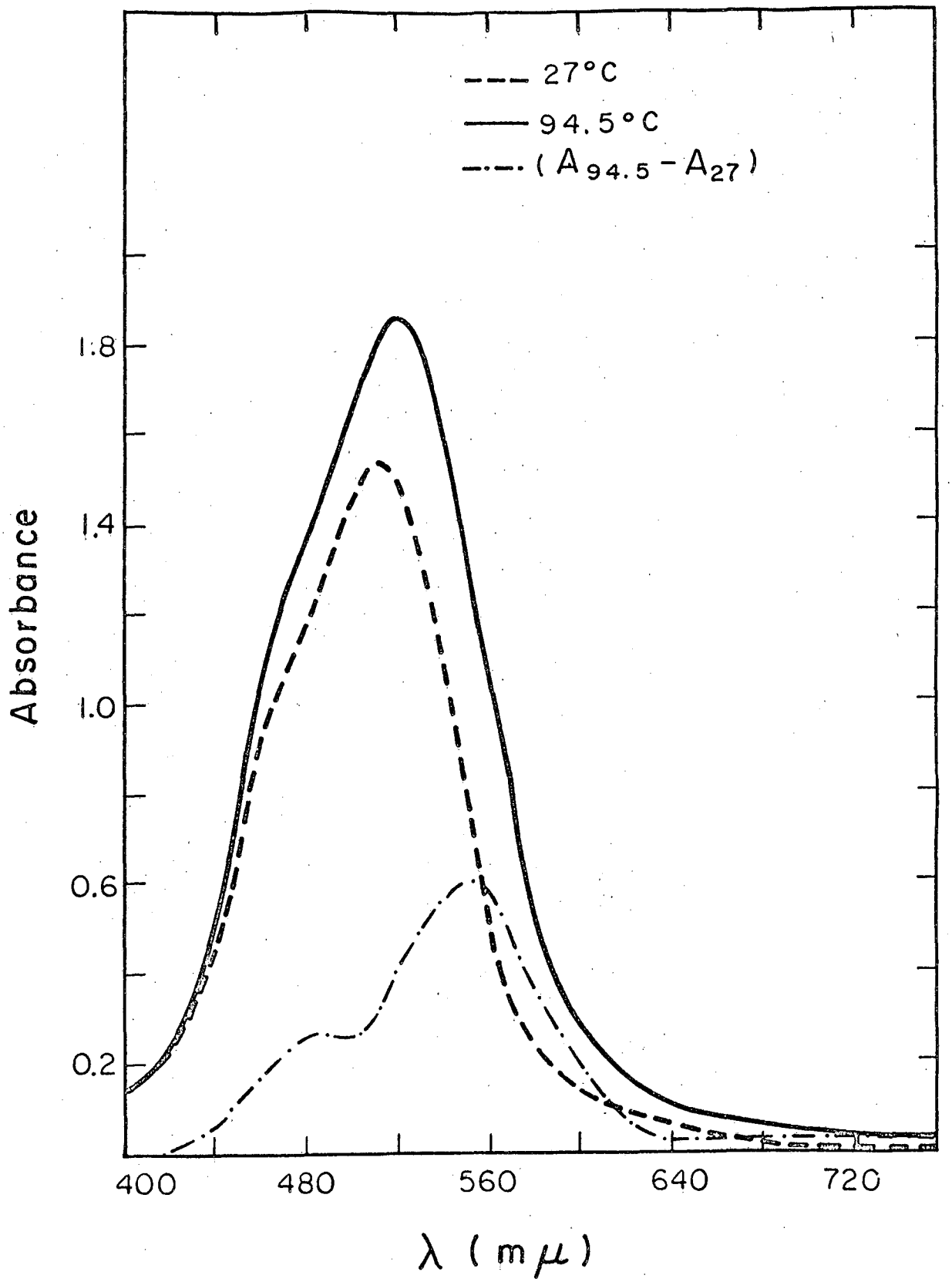

Fig. 8 - Visible spectrum of a 0.600 M $CoSO_4$ solution at 27°C and 94.5°C. Also shown is the curve representing the difference between the two spectra with the density correction from thermal expansion included.

MU-25646

E. Ferrous Ion

Figure 9 shows the large temperature dependence of T_{2p} in solutions of ferrous ammonium sulfate at 5.43 mc. Three solutions of concentrations 1.44×10^{-2}, 6.13×10^{-2}, and 0.377 M were employed. All values shown in Fig. 9 have been corrected to those for a solution which is 1.44×10^{-2} M.

Points were not obtained near 100°C because of the broadening caused by small amounts of Fe^{+3} formed by air oxidation. Much care was taken to exclude air through the use of the sample holder shown in Fig. 1. The solutions were prepared on a vacuum line and the sample holder subsequently filled with an atmosphere of argon. However, the line width due to Fe^{+2} narrows sharply with temperature, while that of Fe^{+3} broadens rapidly.[11] Therefore even a very small amount of Fe^{+3} contributes appreciably to the line width near 100°C.

As with the Co^{+2} solutions the linear region shown in Fig. 9 is most likely 10A. The estimated value[20] of the electron spin relaxation time eliminated 10C from consideration.

Since no chemical exchange controlled region is seen in Fig. 9 it is fortunate that the chemical shift is measurable. It is of the same magnitude as that of the Co^{+2} solutions and is detectable for the same reasons given in the discussion of the Co^{+2} shift. A shift of 119 ppm was observed with a 6.17×10^{-2} M Fe^{+2} solution at 300°K. Table V gives the values of quantities calculated from the chemical shift and from the data of Fig. 9.

The value of τ_{Fe} at 298°K calculated from the chemical shift and the data of Fig. 9 is consistent with the value obtained through curve-fitting on the slight bending at low temperatures in Fig. 9. The straight line for the 10A region calculated from the chemical shift has been inserted in Fig. 9.

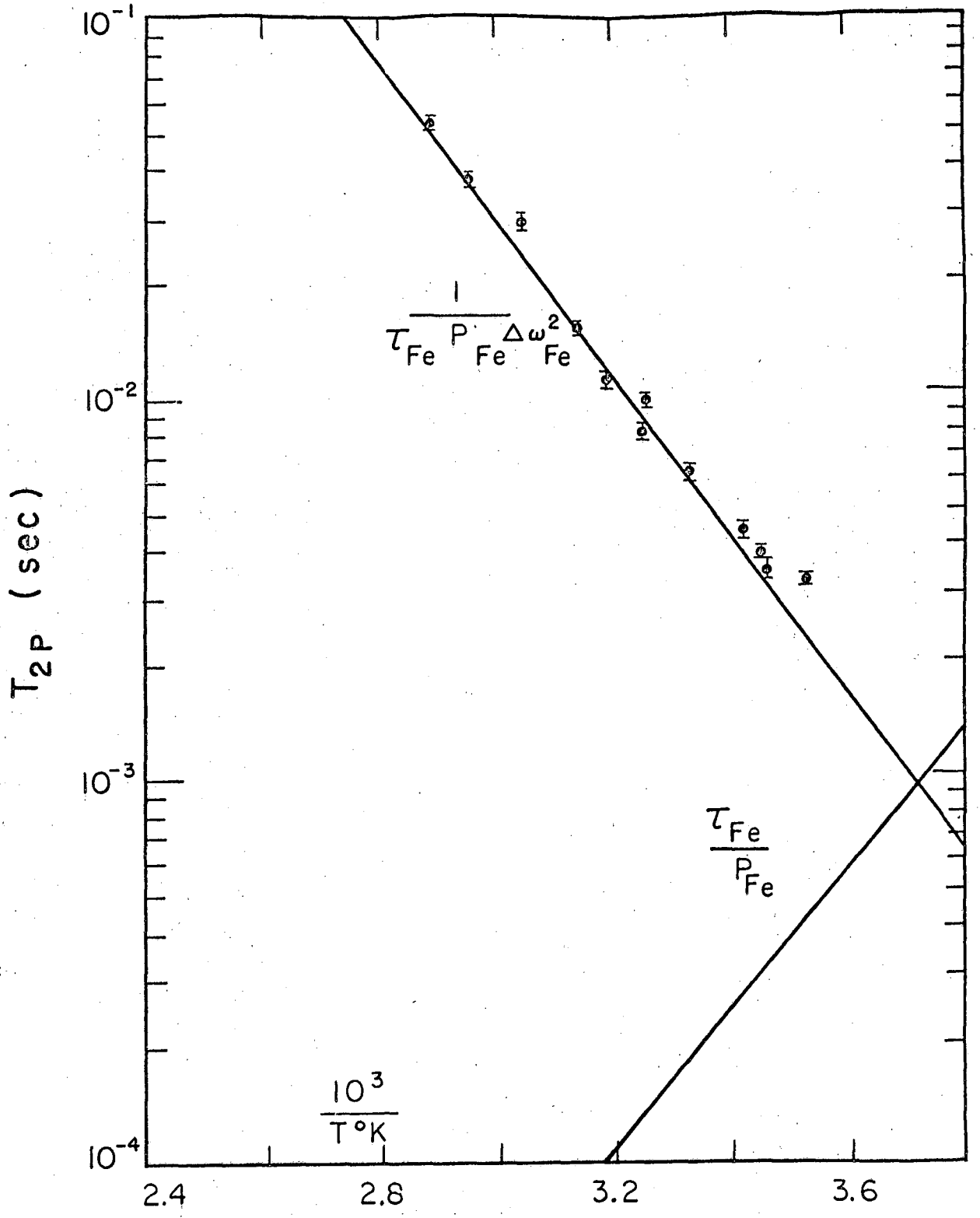

Fig. 9 - Temperature dependence of log T_{2p} of a 1.44×10^{-2} M $Fe(NH_4)_2(SO_4)_2$ solution at 5.43 mc.

MU-25645

TABLE V

Values for the Exchange of Water From the First Coordination Sphere of Ferrous Ion

Quantity	Value
$\Delta H^{\ddagger}$ (kcal)	7.7
k_1 (sec^{-1} at 298°K)	3.2×10^{6}
T_{1e} (sec at 298°K)	$< 1.4 \times 10^{-11}$
A/h (cps)	9.8×10^{5}
$\Delta S^{\ddagger}$ (eu)	-3.0

IV. DISCUSSION

A. Interpretation of O^{17} Results

No other measurements exist for the rates of exchange of water molecules in the first coordination spheres of the cations studied here except for Mn^{+2}, as discussed in the previous section.

An instructive comparison has been made earlier with[16,25,26,2] the rates of a similar process, i.e., the rate of replacement of a water molecule by a sulfate ion in the first coordination sphere of the metal ions. Shown in Fig. 10 is the comparison based now on actual rates of water exchange, rather than lower limits, and on improved sulfate complexing data.[26] The only ion which shows a serious deviation from the linear relationship is Cu^{+2}, and the water exchange rate is known only approximately for this ion. The rough linearity seems to support the thesis[25,27] that the activation energy in complexing reactions arises principally from the partial removal of a water molecule and that bonding to the incoming group is not an important factor. To make the data strictly comparable, the water exchange rates should be corrected by a statistical factor of 3/4, assuming that the incoming group comes from a face of the octahedron.

It is reasonable that the decrease in bonding of the outgoing group is of much more importance to the rate than any weak bonding of the incoming group in the activated complex, but the close correspondence in values of the two sets of rates is indeed remarkable. Possibly the incoming oxygen of the sulfate group behaves much like the oxygen of a water molecule because of the similarity in electric charges. From dipole measurements the charge on oxygen in water is approximately 0.6 of an electronic charge (assuming the positive charge to lie at the protons), while half of an electronic charge would reside on each oxygen of SO_4^{--} if the sulfur is assumed to be neutral. It is interesting that the same

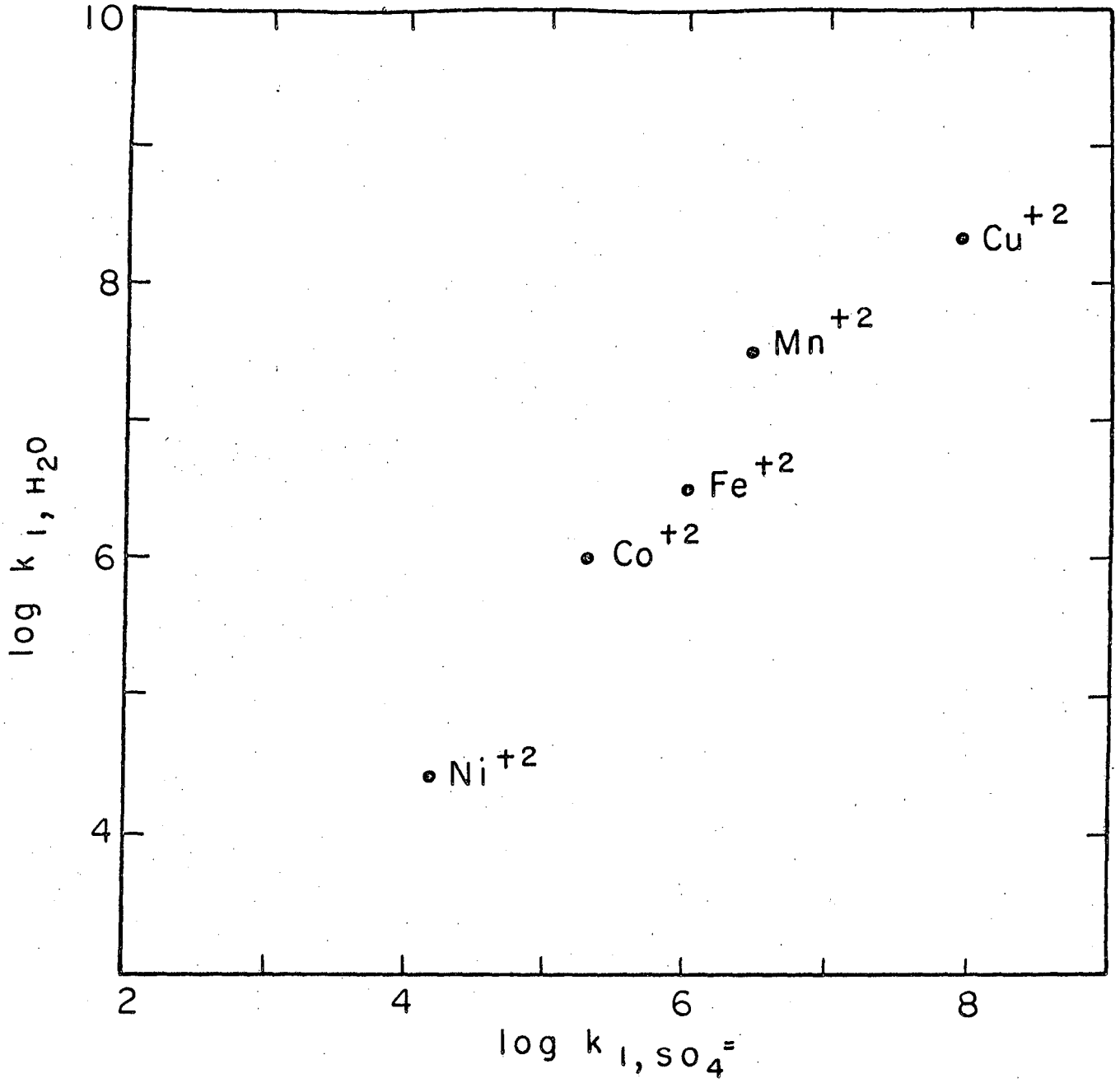

Fig. 10 - Comparison of the rates of water exchange with the rate of replacement of water molecules by sulfate ions in aqueous solutions.

MU-25648

charge distribution would be estimated for the oxygens of the carboxylate ion, which Eigen and coworkers[26] have shown once again to have rates of complexing similar to the sulfate rates.

An attempt was made to correlate the water exchange rates in the solutions of the ions studied with three factors: the electrostatic attraction, the crystal field stabilization, and the extent of covalent bonding between the oxygen and the d electrons of the paramagnetic ion. The purpose was to fix the extent to which these factors contribute to the magnitude of the water exchange rate.

Fig. 11 shows the relationship between the log of the water exchange rates and the second ionization potential[28] of the gaseous metal, with the electron initially in the lowest d level of the singly charged ion. The slow Cu^{+2} exchange rate which is plotted is subject to considerable uncertainty. The plot indicates a rough correlation which would probably be a measure of bonding--both covalent and ionic. It is impossible to separate the correlation for the two types of bonds because the coordinated oxygens penetrate appreciably into the d orbitals of the metal ion and could thus return negative electric charge to the ion either with or without covalent bonding.

Fig. 12 shows the difference in crystal field stabilization[27] between the octahedral complexes of the ions studied and two possible activated complexes for the water exchange process. The theoretical calculations of the crystal field effect were made by Basolo and Pearson[27] in terms of Dq. To obtain the values in kcal shown in Fig. 12 we have employed the experimental spectroscopic values of Dq listed by Basolo and Pearson.[27] It is seen that the resulting predicted crystal field effects are considerably greater than the observed variations in $\Delta H^{\ddagger}$ and $\Delta F^{\ddagger}$. Since effects

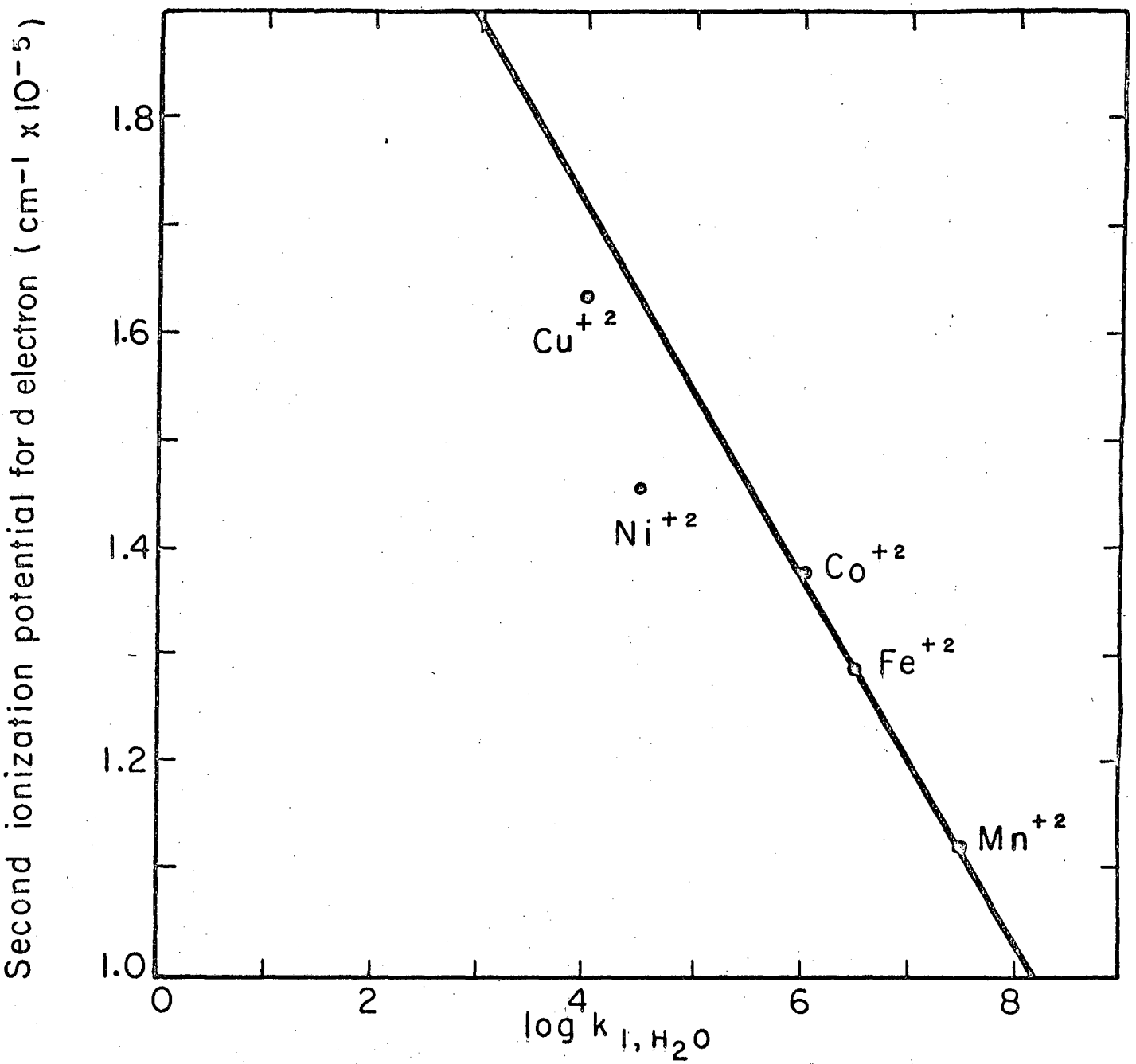

Fig. 11 - Plot of the log of the water exchange rates of the ions studied versus the ionization potential for a d electron in the singly ionized gaseous ion.

MU-25652

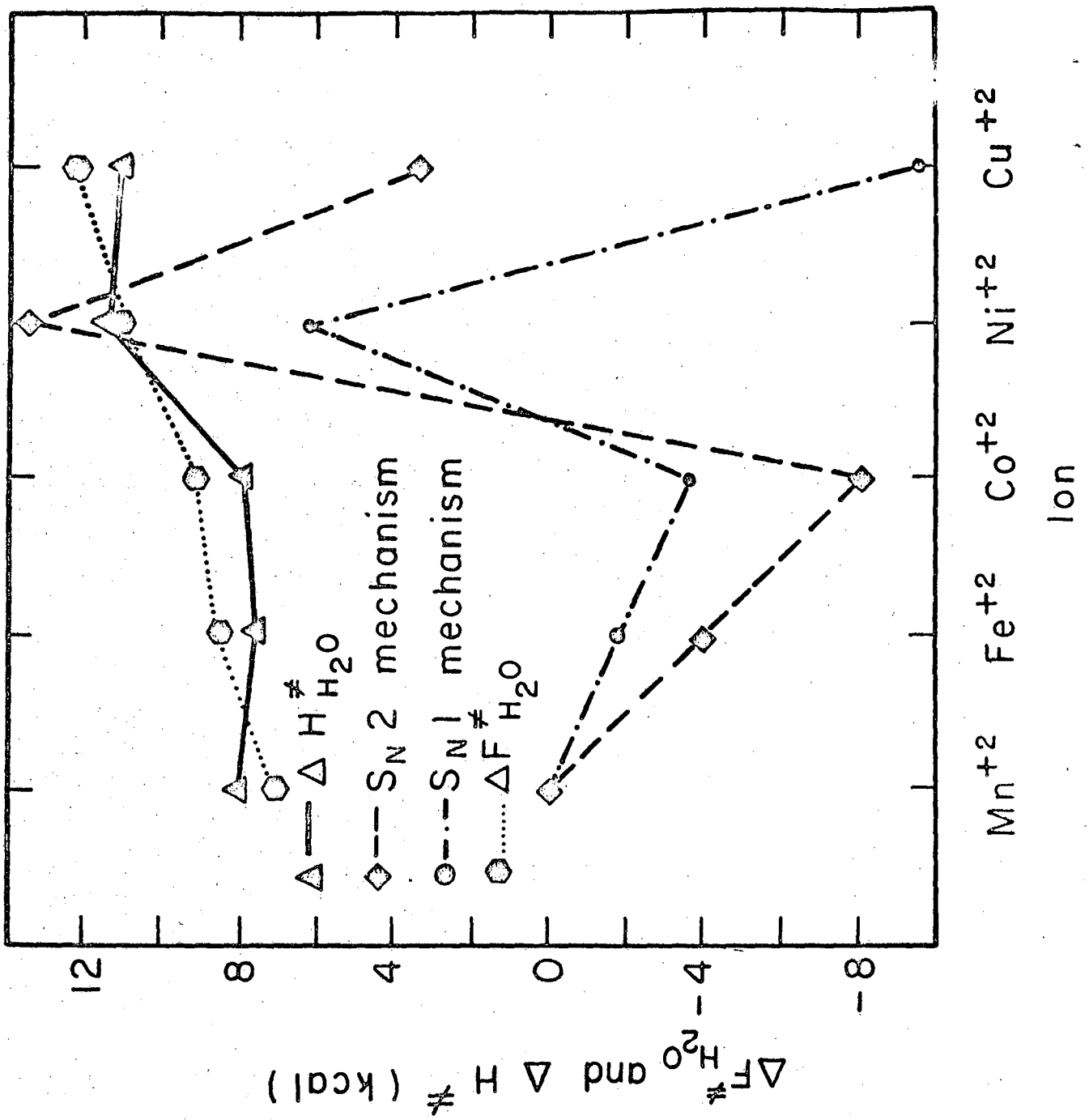

Fig. 12 - Plots of the free energy and enthalpy of activation for the exchange of water molecules and the theoretical enthalpies of activation arising from crystal field effects for two possible activated complexes.

MU-25652

other than crystal field effects will determine the rate parameters, one can hope to see only large, abrupt changes in crystal field trends. Qualitatively the rise in $\Delta H^{\ddagger}$ and $\Delta F^{\ddagger}$ for Ni^{+2}, predicted by crystal field theory for either activated complex, is observed. The heat data indicate a larger effect that the free energy data. Although the free energy data are more precise, a significant part of their variation might be due to entropy changes rather than crystal field enthalpy changes. The magnitude of the effect for Ni^{+2} indicates that even here the major part of $\Delta H^{\ddagger}$ does not arise from crystal field effects. In the case of Mn^{++}, of course, crystal field effects are absent.

Since the gaseous ions have no cyrstal field splitting, the correlation of rate of exchange with ionization potential in Fig. 11 should fail to the extent that crystal field effects operate. As predicted the rate for Ni^{+2} deviates toward a smaller value from that obtained by the extrapolation of the straight line through Nm^{+2}, Fe^{+2}, and Co^{+2}.

An attempt was made to account for the magnitude of the observed rate on the basis of a primitive electrostatic model in which only the removal of the outgoing water is considered. Using the formula for the electrostatic attraction between a dipole and a charge one calculates the free energy of activation from this source for a divalent ion to be:

$$\Delta F_e^{\ddagger} = -252\ (1/d_{\ddagger}^2 - 1/d^2)/D \text{ kcal} \qquad (21)$$

where D is the effective dielectric constant and d and $d_{\ddagger}$ are the metal to oxygen distances in $\mathring{A}$ of the water in the hydrated ion and activated complex, respectively. Taking d for Mn^{+2} to be 2.20 $\mathring{A}$ one calculates that $d_{\ddagger}$ - d would have to be ca. 0.3 $\mathring{A}$ to yield the observed $\Delta F^{\ddagger}$ of 7.2 kcal, with the dielectric constant having the optical value for water, i.e., 1.77. It is seen that such a model can account for the magnitude of the

activation energy, although the appropriateness of the assumed small dielectric constant is open to cricicism.

The change of $\Delta F^{\ddagger}$ with size of the metal can be estimated for the above model assuming that the $d_{\ddagger}$ - d is constant at 0.3 Å. The calculated change with radius is only about one third of the observed value, even making a correction for crystal field effects, but this may well be only a reflection of the inadequacy of the model. Particularly the assumption of constant stretching is open to question and a more realistic model would probably improve the comparison.

The coupling constants calculated from the water exchange data are dependent on covalent bonding between the oxygen and the d electrons of the paramagnetic ion. There is no apparent correlation between these coupling constants and the rates. The conclusion is that covalent character measured by the coupling constants does not dominate the energy of the activated complex.

In summary, the observations are consistent with an appreciable crystal field effect on the rate of exchange. No definite evidence for covalent bonding effects was found, apart from crystal field contributions, which might be so interpreted. The magnitude of the rates can be accounted for by a crude electrostatic model; this interpretation is possible but by no means necessary. Regarding covalent bonding effects it is of interest that Eigen[26] reports the first order rate constants for sulfate complex formations of Mg^{++} and Ni^{++} to be 1×10^{5} and 1×10^{4} sec^{-1} respectively. Since the empirical ionic radii[29] of the two ions are nearly the same, i.e., 0.75 and 0.74 Å respectively, it must be concluded that covalent effects in Ni^{++} are not large relative to Mg^{++}. The ten fold lower rate for Ni^{++} can probably be attributed to crystal field effects.

One further correlation is shown in Figures 13 and 14. Fig. 13 shows a plot of the log of the water exchange rates versus the first stability constant for the coordination of ethylenediamine[30,31] with the paramagnetic ions studied. There is rather good correlation between complex stability and rate of exchange, as might be expected. The plot shows a deviation for Co^{+2}. This suggests that perhaps Co^{+2} exists in solution as a slightly distorted octahedron; however this is shown to be not the case in Fig. 14. Here the same deviation appears in the data for the formation of the third complex. but octahedral distortion should affect the stability of the third complex in the opposite direction to that of the first.

B. Consideration of Proton Results

It is interesting to compare the NMR data on dilute aqueous solutions of paramagnetic ions from the present O^{17} work and the proton studies of other authors.[4,12,32] For each ion studied here, a plot has been made (Figs. 15 through 19) of log P T_{2p} vs. $10^3/T$, so that both O^{17} and proton data are on the same plot.

The comparisons represented in Figs. 15 through 19 are given in part as a check on the consistency of the assumptions previously made by the author and by those who have studied the proton resonance. One further calculation must be made, however, before the results can be compared.

In the cases of each of the five ions studied here the proton results yielded values of the dipole - dipole relaxation times as a function of temperature. It is of considerable interest to consider the ratio of the dipole - dipole relaxation times for protons and O^{17} in the same solution of a paramagnetic ion. The following is a very crude attempt at the calculation of such a ratio. According to the equation of Solomon[7] the ratio is

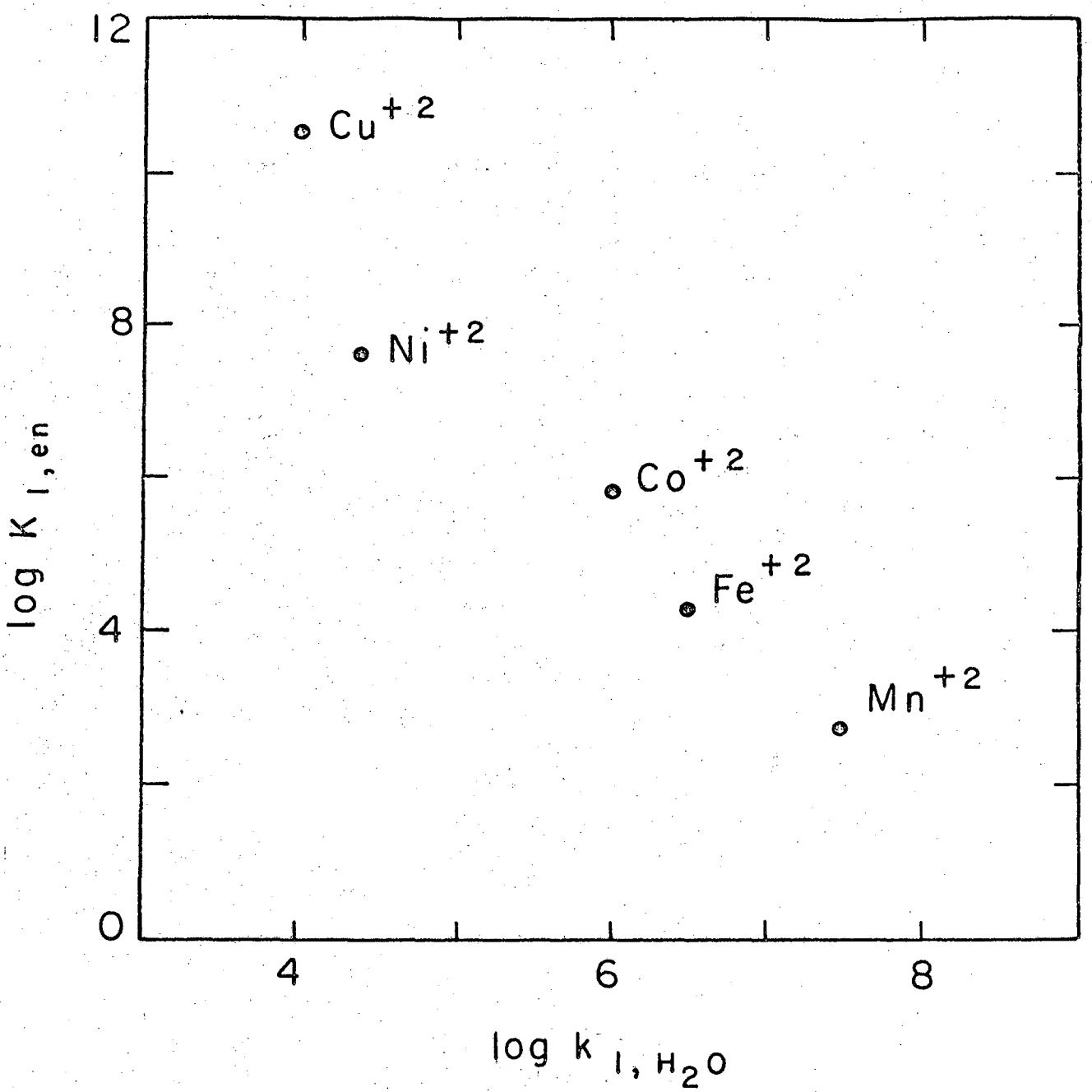

Fig. 13 - Logarithmic plot of the water exchange rates versus the first formation constants for the paramagnetic ion-ethylene-diamine system.

MU-25650

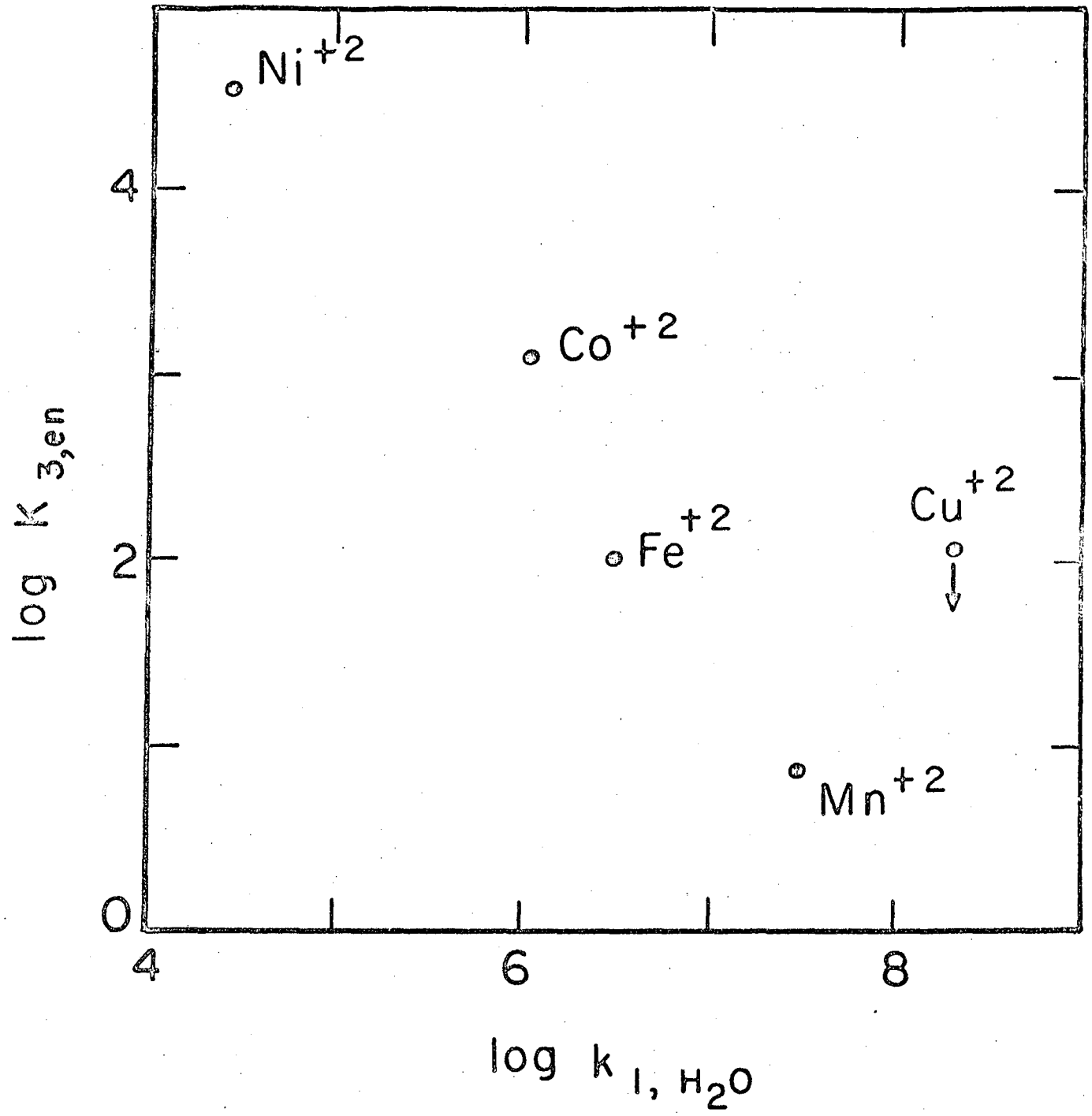

Fig. 14 - Logarithmic plot of the water exchange rates versus the third formation constant for the paramagnetic ion-ethylene-diamine system. The Cu^{++} point is only an upper limit.

MU-25650

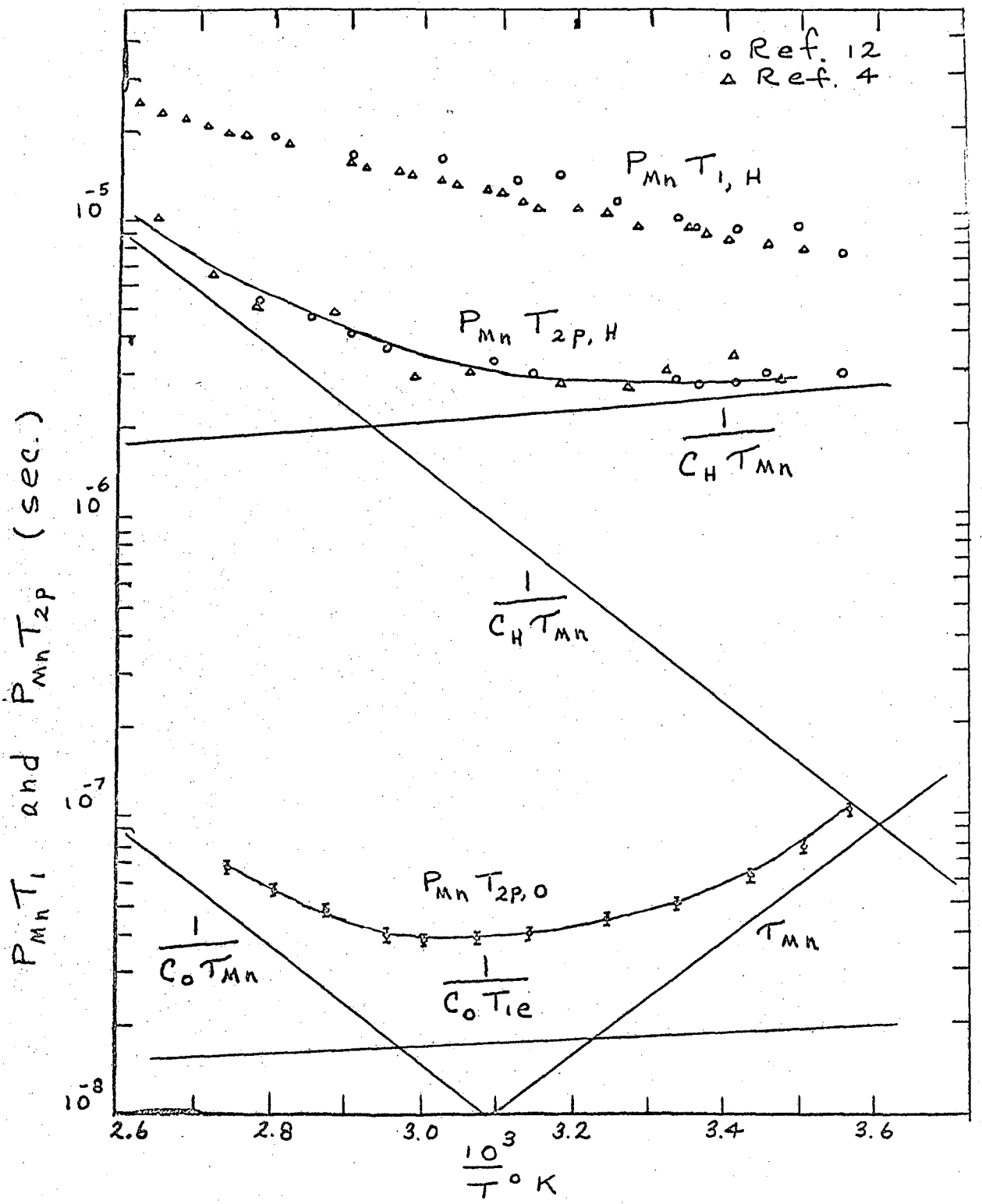

Fig. 15 - A plot of $P_{Mn}T_{2p}$ for Mn^{+2} solutions from the present O^{17} NMR and from the proton NMR data.[4,12] Also shown are the experimental T_1's obtained in the proton studies. The lines which resulted from the curve-fitting of the O^{17} data are shown, along with the corresponding lines calculated for protons.

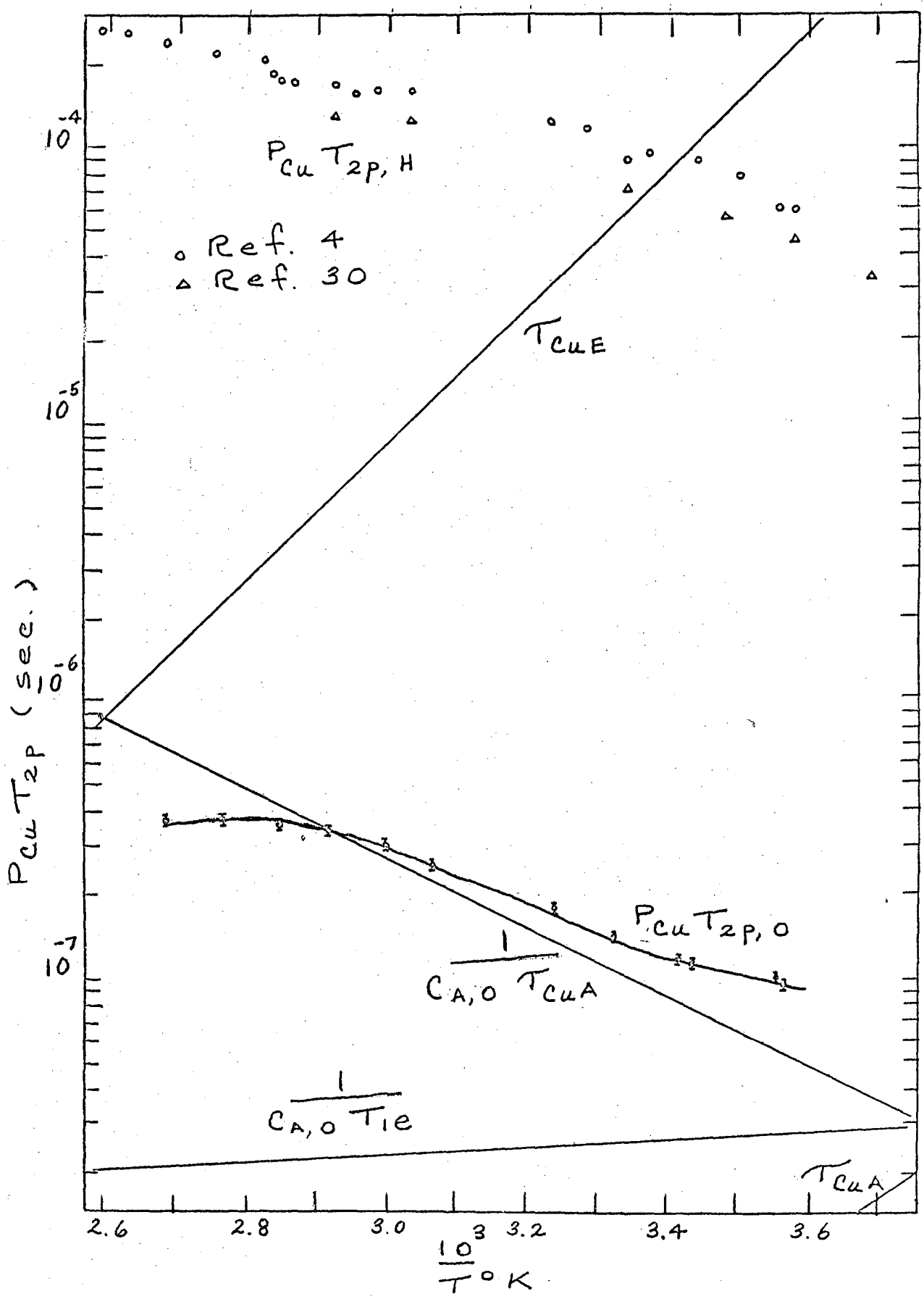

Fig. 16 - A plot of $P_{Cu} T_{2p}$ for Cu^{+2} solutions, showing O^{17} and proton[4,32] NMR results.

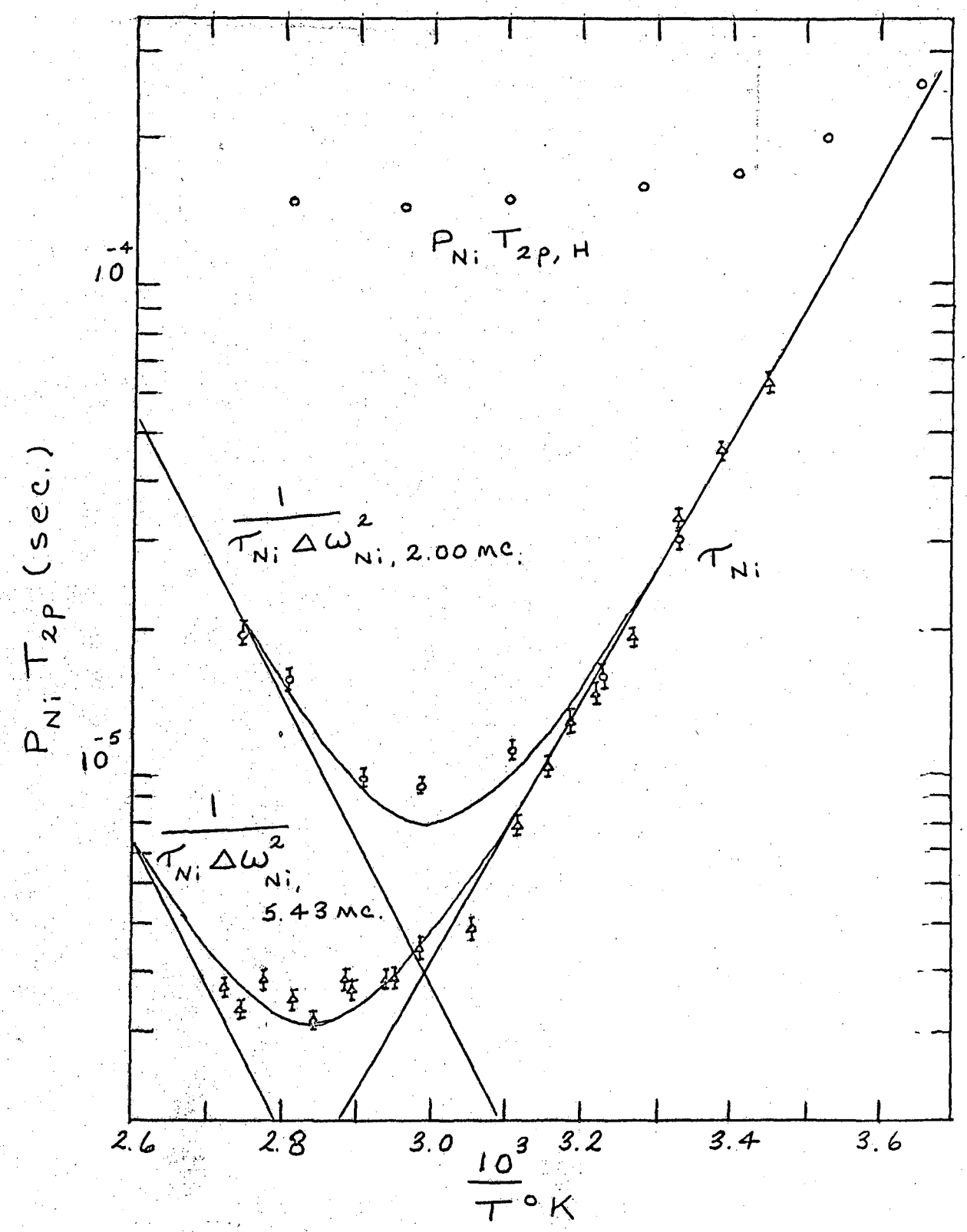

Fig. 17 - A plot of $P_{Ni}\,T_{2p}$ for Ni^{+2} solutions from the O^{17} data and from proton NMR data.[32]

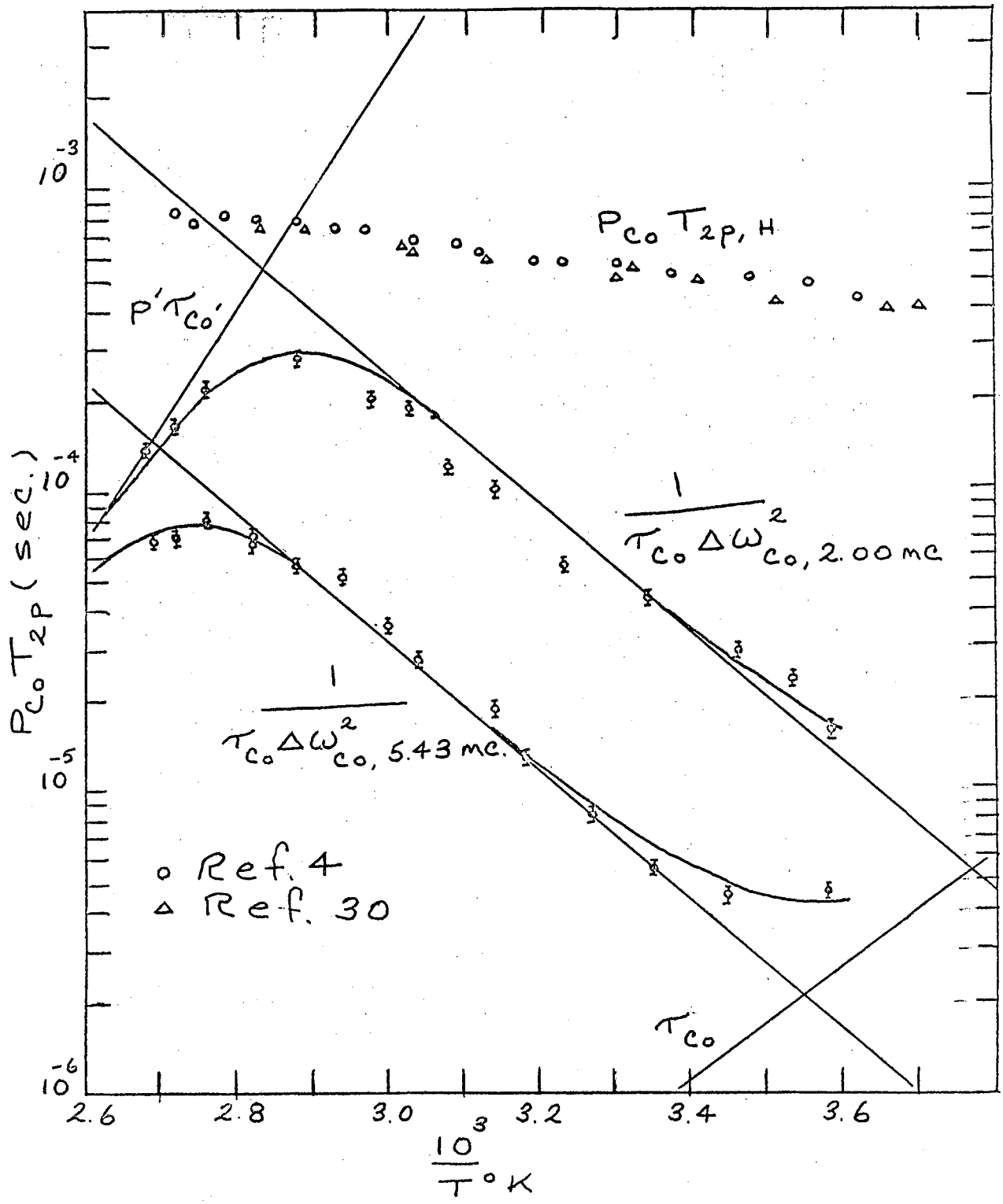

Fig. 18 - A plot of $P_{Co}\ T_{2p}$ for Co^{+2} solutions calculated from O^{17} data and results of proton NMR.[4,32]

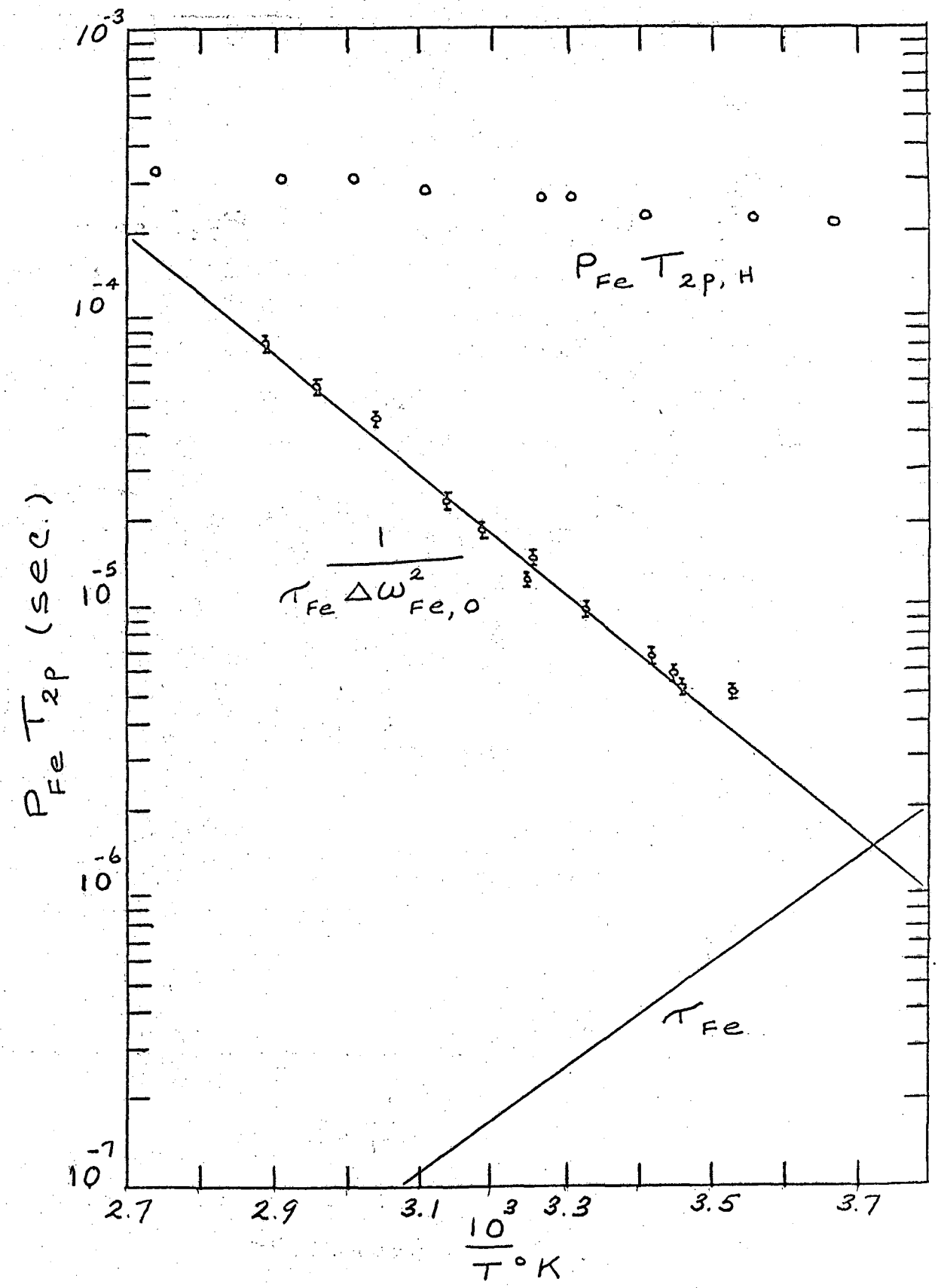

Fig. 19 - A plot of $P_{Fe}\ T_{2p}$ for Fe^{+2} solutions using O^{17} and proton[32] data.

$$T_{2H}/T_{20} = \frac{I_H (I_H + 1) \gamma_O^2 \; r_H^6}{I_O (I_O + 1) \gamma_H^2 \; r_O^6}$$

where r_H and r_O are the distances between the proton and the O^{17} nucleus respectively and the paramagnetic electrons. The assumption is made that the correlation times for proton motion and O^{17} motion are the same, although this may possibly be erroneous.

For purposes of calculation the paramagnetic ion is considered to have its paramagnetic electrons centered at the nucleus. The M - O - H bond was taken to be the tetrahedral angle, $109^{0}25'$, in the coordinated state. X-ray crystal studies[33] have indicated that such is the case. The H - O bond distance is taken to be 0.96 Å, the value for uncoordinated water. The M - O bond distances were taken to be the crystalline internuclear distances.[29]

The result of this calculation is that the dipole - dipole relaxation mechanism is ca. 0.8 times as effective for O^{17} as for protons

The application of this result as well as the results of other comparisons between O^{17} and proton data are given in the following separate considerations of each ion.

1. Manganous Ion

Fig. 15 shows the fitted O^{17} data along with the data of Bernheim et al.[4] and Bloembergen and Morgan.[12] The values of $P_{Mn}T_{1H}$ are included in order to show the magnitude of the dipole - dipole relaxation for protons and for purposes of comparison with the scalar coupling relaxation. The lines representing $1/C_H\tau_{Mn}$ and $1/C_HT_{1e}$ have been drawn through a consideration of the corresponding lines for O^{17} together with the following facts and assumptions. The O^{17} work was done at 5.43 mc, while the proton results were obtained at 10 mc[4] and 14 mc.[12] The consequence of this

frequency difference, according to Eq. (22) of Bloembergen and Morgan,[12] is the slightly larger slope of the line for $1/C_H T_{1e}$ over that for $1/C_O T_{1e}$. Also T_{1e} at the proton frequencies is calculated to be ca. 0.7 of the value at the O^{17} frequency. The value of the constant C is given by

$$C = 4/9\ I\ (I + 1)\ S\ (S + 1)\ (A/\hbar)^2$$

where I for protons is 1/2 and for O^{17} is 5/2. $A/\hbar$ was taken to be 1.0×10^6 cps for protons, as found by Bloembergen and Morgan.[12] The mechanism of proton exchange was assumed to be the exchange of whole water molecules. Therefore τ_{Mn} is the same for both O^{17} and protons and the chemical exchange line drawn applies to both cases.

Figure 15 shows that the oxygen and proton results are in good agreement.

2. Cupric Ion

Figure 16 shows the O^{17} data and the proton data of Bernheim et al.[4] and of Hauser and Laukien.[32] The O^{17} data were plotted, assuming a coordination number of two. A coordination number of six was used in plotting proton results. The O^{17} results have been interpreted previously in this thesis as arising from interactions at the axial positions. The choice of six as the coordination number appropriate for the proton results can be explained through the following considerations.

Since $T_1 \cong T_2$ for the proton results, it has been concluded[4,32] that the values shown arise from dipole-dipole relaxation. The line representing exchange at the equatorial positions cuts the proton data. To the high temperature side of the τ_{CuE} line, the proton relaxation should be the sum of that at the equatorial and axial positions and the effective coordination number is six. To the right of the τ_{CuE} line, however, the

relaxation at the equatorial positions is chemical exchange controlled. Consequently, the effective coordination number becomes two at low temperatures. This is apart from the fact that the inherent relaxation at the two positions is probably not the same. The bond distances alone would indicate this. The data of Fig. 16 should show roughly a three fold increase superimposed upon the sloping line as the region of the line τ_{CuE} is traversed from left to right.

The data show a small tendency toward the expected S shape, but not nearly as large as is expected. This may be explained by means of the following considerations. The tumbling time which governs the relaxation may well have a temperature dependence similar to that of pure water. This would include a sharp increase in the temperature region from 20°C to 0°C. Such a sharp increase in τ_c would partially or totally cancel out the increase in T_{2H} due to the change in effective coordination number. The data then are possibly consistent with predictions.

Two paths are open to the explanation of the data even if the correlation time argument is not used. Either the increase should not be present at the crossover or the line τ_{CuE} is in error and should have been drawn so as to give no crossover in the observed temperature region.

The first case would occur only if the inherent relaxation at the equatorial positions were much smaller than that at the axial positions. Since the axial waters are much more loosely bonded this is unlikely.

The second explanation is plausible, however. The slope of the τ_{CuE} line is very uncertain and could be made much smaller. The smaller slope would then probably be consistent with the inversion process discussed previously in this thesis.

From the proton data of Fig. 16, one predicts no significant dipole - dipole contribution to the observed relaxation of O^{17}, in agreement with the O^{17} T_1 results.

From the O^{17} results one predicts that the proton relaxation should occur largely through scalar coupling if the ratio of proton to oxygen scalar coupling constants is about the same as with manganous ion. Since scalar coupling is not important with protons the manganous ion coupling constant ratio is not generally applicable. It is possible that a significant amount of proton-electron coupling is done through bonding between the unpaired electrons in the Eg level of the paramagentic ion and the H - O bond electrons. Such an interaction would be largest in Mn^{+2} and zero in Ni^{+2} and Cu^{+2}. The effect of an error in estimation of the coupling constant ratio is intensified in the relaxation since the ratio enters squared.

3. Nickelous Ion

Fig. 17 shows the O^{17} results at 5.43 mc and 2.00 mc and the proton data of Hauser and Laukien.[32] T_1 of the proton was very nearly equal to T_2 and hence the relaxation was assumed[32] to occur through the dipole - dipole mechanism. The plot definitely shows that the bend at low temperatures for the proton data is due to chemical exchange from the first coordination sphere. An attempt was made to fit the proton data through the following considerations.

The high temperature slope of the nickel data is small. The O^{17} results discussed previously have shown that the electronic T_1 for Ni^{+2} is quite possibly shorter than the tumbling correlation time, τ_c. In such a case the dipole - dipole relaxation may be governed by T_{1e} rather than τ_c. The slope of the dipole - dipole relaxation line was taken to be the same as the T_{1e} slope of Mn^{+2}. All dipole - dipole relaxation is presumed to occur in the first coordination sphere. The result of the curve-fitting shows that the data do not bend up sharply enough at low temperatures.

This may be explained by assuming that a small amount of dipole - dipole relaxation occurs outside the first coordination sphere. This relaxation is not interrupted by τ_{Ni} and tends to round off and limit the observed bend. The ratio of second coordination sphere relaxation to that which occurs in the first coordination sphere may be estimated through the use of the following model.

The comparison is made between the relaxation of the six first coordination sphere waters and the eight waters situated in the faces of the octahedron. The M - O internuclear distances are the crystalline distances used previously in this thesis. The O - O distance can never be less than twice the van der Waals' radius for oxygen. This radius is taken to be 1.4 Å.

The Solomon equation[7] yields for the ratio of relaxation times:

$$\frac{T_{2,\ 2nd}}{T_{2,\ 1st}} = 6/8\ \frac{r_{2nd}^{6}}{r_{1st}^{6}}$$

For Ni^{+2} the ratio is 17.5. There is considerable uncertainty in this value due to a questionable assumption used in the equation above. This is the assumption that the correlation times for the first and second coordination spheres are the same. There is also considerable uncertainty in fitting the data with this additional parameter; however, the value of 17.5 is not inconsistent with the results.

From the O^{17} results one predicts that scalar coupling should make a sizeable contribution to the proton relaxation at low temperatures if the coupling constant ratio of 2.7 for manganous protons to oxygens applies. The fact that such is not the case experimentally may be explained by means of the coupling constant argument advanced for Cu^{+2}.

The dipole - dipole contribution to O^{17} relaxation is predicted to be small and unresolvable from the scalar coupling contribution on the basis of Fig. 17.

4. Cobaltous Ion

Fig. 18 shows the O^{17} results at 5.43 and 2.00 mc along with the proton date of Bernheim et al.[4] and Hauser and Laukien.[32] Again T_{1H} is approximately equal to T_{2H} and the relaxation process is[4,3] assumed to be dipolar. The plot reveals that there could be a sizeable dipole - dipole contribution to the O^{17} relaxation in the high temperature bendover region at 2.00 mc. The presence of such a contribution does not alter the fact that the presence of a new cobalt species is indicated. The dipole - dipole contribution cannot produce the rapid decrease with temperature of T_{2p} for O^{17} observed at the highest temperature but would yield a slope of the opposite sign. All arguments based on the slope of the P_{Co}, τ_{Co}, line are then extremely uncertain. The uncertainty introduced into the enthalpy of activation for water exchange from the octahedral species by the dipole contribution is not sizeable, however, as the enthalpy was best determined from the 5.43 mc data, where dipole - dipole effects play a very small part.

Fig. 18 shows the high temperature chemical exchange line cutting through the proton data. There is no observable break in the $P_{Co}T_{2p,\ H}$ curve at the intersection. This is consistent with the earlier assumption that the new cobalt species is present as a minor component. If the inherent dipole - dipole relaxation on the new species is comparable to that on the octahedral species, the ratio of the contributions to the total relaxation of protons will be the ratio of the concentrations of the two species. If the new species is present in a small concentration, the fact that its contribution to relaxation falls off rapidly as the temperature is lowered leaves the total observed relaxation virtually unaffected.

5. Ferrous Ion

Fig. 19 gives the O^{17} data and the proton data of Hauser and Laukien.[32] T_{1H} is equal to T_{2H} and the relaxation of protons has again been assigned to the dipolar mechanism. From the proton data one predicts a sizeable contribution of dipole - dipole relaxation for O^{17}. This result casts a small degree of uncertainty on the value given for $\Delta H^{\ddagger}_{H_2O}$. Ferrous ion does offer the opportunity, however, to obtain experimentally a value for the dipole - dipole contribution to O^{17} relaxation. If the production of Fe^{+3} can be surpressed near 100°C, a bendover should occur in T_{2p} due to the dipole contribution

The O^{17} data lead one to predict that there is no important scalar coupling contribution to proton relaxation.

ACKNOWLEDGMENTS

I wish to express my most sincere gratitude to Professor Robert E. Connick, whose patient counsel has contributed immeasurably to this work. I also wish to thank Professor Rollie Myers for his many helpful suggestions. I am grateful to Dr. Juana V. Acrivos, Dr. Charles Sederholm, and Mr. Frank Papen for their assistance with electronic equipment. Finally I wish to acknowledge my fellow graduate students for their many helpful suggestions.

Financial support was received from the U. S. Atomic Energy Commission through the Lawrence Radiation Laboratory.

APPENDICES

A. Experimental Data

Table A-1. The T_2 and T_1 of 1.2% O^{17} H_2O as a function of temperature. The water is also 0.1 M in $HClO_4$ and is ca. 25 mole percent in deuterium.

$10^3/T^oK.$	Line width[a]	$T_2 X 10^3$ (sec.)	H_{1s}[b]	$T_1 X 10^3$ (sec.)
2.800	17.95	8.85	.0540	11.03
3.060	23.50	6.76	.0728	7.97
3.333	30.40	5.23	.0998	5.47
3.445	37.30	4.26		
3.510	43.7	3.64		
3.550	50.6			

[a] All line widths in this appendix refer to the half width at half height in cycles per second and are the average of several observed values.

[b] The value of the radio frequency field in gauss where the peak height is a maximum in the plot of peak height vs. rf field.

Table A-2. T_1, T_2 and T_{2p} of a 1.82 X 10^{-4} M $MnSO_4$ solution in 0.10 M $HClO_4$ as a function of temperature.

$10^3/T^oK.$	Line width	T_2X10^3	$T_{2,H2O}X10^3$	$T_{2p}X10^3$	H_{ls}	T_1X10^3 [a]
2.745	63.9	2.49	9.25	3.41	.0886	14.56
2.800	73.6	2.16	8.85	2.86		
2.870	85.0	1.87	8.20	2.42	.1060	13.55
2.950	102.5	1.55	7.55	1.95		
3.000	107.5	1.48	7.20	1.86	.1365	10.33
3.070	106.0	1.50	6.70	1.93		
3.140	105.5	1.51	6.25	1.99	.1450	8.98
3.240	97.0	1.64	5.70	2.30	.1528	7.43
3.333	91.4	1.74	5.23	2.61	.1638	6.11
3.430	86.0	1.85	4.40	3.19		
3.500	82.4	1.93	3.70	4.03		
3.570	80.8	1.97	3.10	5.38		

[a] All relaxation times are expressed in seconds.

Table A-3. T_1, T_2 and T_{2p} of a 1.00 X 10^{-3} M Cu $(NO_3)_2$ solution in 0.10 M $HClO_4$ as a function of temperature. Also shown is an approximate T_1 and T_2 determination with a 5.00 X 10^{-3} M $CuSO_4$ solution in 0.10 M $HClO_4$ using the derivative method.

$10^3/T^oK$	Line width	T_2X10^3	$T_{2,H_2O}X10^3$	$T_{2p}X10^3$	H_{1s}	T_1X10^3	Soln.[a]
2.690	31.0	5.13	9.80	10.8			A
2.770	32.6	4.88	9.10	10.5			A
2.850	33.5	4.57	8.40	10.0			A
2.920	37.1	4.28	7.80	9.53	.0890	8.39	A
3.005	40.8	3.89	7.15	8.54			A
3.070	45.2	3.52	6.75	7.35	.1053	7.30	A
3.245	59.8	2.66	5.70	5.00			A
3.333	71.0	2.24	5.23	3.96	.1510	5.58	A
3.420	84.2	1.89	4.50	3.26			A
3.435	86.9	1.83	4.35	3.15			A
3.560	108.2	1.47	3.10	2.79			A
3.333	~225.	~ 0.7	5.23	~0.8	~.15	~5	B

[a] Solution A is 1.00 X 10^{-3} M Cu $(NO_3)_2$ and solution B is 5.00 X 10^{-3} $CuSO_4$.

Table A-4. T_2 and T_{2p} of $Ni(NO_3)_2$ solutions in 0.10 M $HClO_4$ as a function of temperature and frequency.

$10^3/T^oK.$	Half width	$T_2 X10^3$	$T_{2,H_2O} X10^3$	$T_{2p} X10^3$	Solution[a]
		At. 5.43 mc			
2.730	45.2	3.52	9.40	5.65	A
2.745	48.0	3.31	9.30	5.15	A
2.780	45.2	3.52	9.00	5.78	A
2.820	48.0	3.31	8.60	5.37	A
2.855	52.2	3.05	8.35	4.81	A
2.895	46.7	3.405	8.00	5.92	A
2.900	48.6	3.275	8.00	5.55	A
2.945	48.0	3.31	7.60	5.88	A
2.955	46.4	3.42	8.35	5.81	A
2.975	153.0	1.038	7.40	1.21	B
3.050	119.5	1.33	6.85	1.65	B
3.125	97.3	1.635	6.40	2.17	B
3.160	80.7	1.95	6.20	2.88	B
3.190	158.	1.005	6.00	1.21	C
3.225	142.5	1.115	5.80	1.38	C
3.265	117.3	1.355	5.55	1.79	C
3.333	81.4	1.955	5.23	3.11	C
3.390	70.7	2.25	4.75	4.27	C
3.455	64.9	2.45	4.20	5.88	C
		At 2.00 mc			
2.750	34.8	4.57	9.25	9.00	D
2.810	40.6	3.92	8.70	7.14	D
2.910	55.3	2.87	7.90	4.52	D
2.995	58.0	2.74	7.25	4.40	D
3.110	54.3	2.93	6.45	5.38	D
3.230	48.6	3.27	5.75	7.58	D
3.333	41.8	3.80	5.23	1.39	D

[a] Solution A is 6.12×10^{-3} M, solution B is 3.39×10^{-2} M, solution C is 0.100 M, and solution D is 0.0200 M.

Table A-5. T_2 and T_{2p} of $CoSO_4$ and $Co(ClO_4)_2$ solutions in 0.10 M $HClO_4$ as a function of temperature and frequency.

$10^3/T^oK.$	Line width	T_2X10^3	$T_{2,H_2O}X10^3$	$T_{2p}X10^3$	Solution[a]
		At 5.43 mc			
2.690	57.0	2.79	9.80	3.91	A
2.820	60.4	2.63	8.65	3.79	A
2.880	68.8	2.31	8.15	3.22	A
2.940	36.4	4.37	7.65	10.2	B
3.050	52.3	3.04	6.85	5.46	B
3.140	68.2	2.33	6.30	3.72	B
2.720	52.1	3.05	9.55	4.48	C
2.755	48.3	3.29	9.20	5.12	C
2.820	53.9	2.95	8.65	4.48	C
3.000	93.7	1.70	7.20	2.24	C
3.180	39.6	4.02	6.05	11.9	D
3.270	49.5	3.21	5.50	7.75	D
3.350	61.8	2.57	5.05	5.23	D
3.450	76.0	2.09	4.20	4.17	D
3.580	94.0	1.69	2.80	4.25	D
		At 2.00 mc			
2.680	33.4	3.67	9.90	5.84	E
2.725	39.7	4.00	9.55	6.89	E
2.760	34.4	4.62	9.15	9.34	E
2.880	33.4	4.77	8.15	11.40	E
2.980	40.0	3.97	7.35	8.62	E
3.080	54.4	2.92	6.70	5.18	E
3.030	29.6	5.37	7.00	22.9	F
3.140	37.6	4.22	6.30	12.8	F
3.250	51.4	3.09	5.65	6.85	F
3.340	61.0	2.60	5.10	5.31	F
3.460	82.8	1.92	4.10	3.61	F
3.530	102.3	1.555	3.40	2.86	F
3.580	137.5	1.155	2.80	1.965	F

[a] Solution A is .163 M $CoSO_4$, solution B is 0.0477 M $CoSO_4$, solution C is 0.147 M $Co(ClO_4)_2$, solution D is 0.100 M $CoSO_4$, solution E is 0.223 M $CoSO_4$, and solution F is 0.0763 M $CoSO_4$.

Table A-6. T_2 and T_{2p} of $Fe(NH_4)_2(SO_4)_2$ solutions in 0.10 M $HClO_4$ as a function of temperature.

$10^3/T^oK$	Line width	$T_2 X10^3$	$T_{2,H_2O} X10^3$	$T_{2p} X10^3$	Solution[a]
2.895	98.0	1.62	8.00	2.03	A
2.955	130.0	1.22	7.55	1.45	A
3.045	46.3	3.43	6.90	6.85	B
3.140	70.7	2.25	6.30	3.51	B
3.190	83.3	1.91	6.00	2.81	B
3.250	104.0	1.53	5.65	2.10	B
3.255	98.5	1.615	5.60	2.27	B
3.333	138.0	1.153	5.23	1.48	B
3.420	71.3	2.23	4.50	4.42	C
3.450	76.5	2.08	4.25	4.06	C
3.460	84.5	1.88	4.15	3.43	C
3.530	94.7	1.68	3.40	3.33	C

[a] Solution A is 0.377 M, solution B is 0.0613 M, and solution C is 0.0144 M.

B. Expanded Steady State Solution of the Bloch Equations, Modified to Include Chemical Exchange.

The solution given here is intended to present in detail the mathematics leading to Eqs. (7) and (8). Since it is not difficult to extend to n species the case in which the minor species exchange only with the solvent, the treatment will be of such a case.

The solution of interest contains the nucleus observed in n different environments. One of these, a, is present in a much higher concentration than the others taken collectively. Chemical exchange is allowed between a and each of the n-1 minor environments. Direct interconversion among the n-1 states is not allowed, however. The conditions of slow passage and low power level are employed. The definition of terms in the following modified Bloch equations is a simple extension of those given in Part I.

$$
\begin{array}{lccccccccc}
 & -A\,G_a & + & G_b/\tau_{ba} & + & G_c/\tau_{ca} & + \cdots\cdots + & G_n/\tau_{na} & = & i\omega_1 M_0^a \\
\text{B-1} & G_a/\tau_{ab} & - & B\,G_b & & & & & = & i\omega_1 M_0^b \\
 & G_a/\tau_{ac} & & & - & C\,G_c & & & = & i\omega_1 M_0^c \\
 & \vdots & & & & \vdots & & & & \\
 & G_a/\tau_{an} & & & & & & -N\,G_n & = & i\omega_1 M_0^n
\end{array}
$$

The solution of these equations for G is best accomplished through the use of determinants. The result is the following.

$$G = -i\omega_1 \left\{ M_0^a \prod_{j=b}^{n} J + \sum_{j=b}^{n} M_0^j \prod_{l=b,\, l\neq j}^{n} L_l / \tau_{ja} + \sum_{j=b}^{n} A\, M_0^j \prod_{l=b,\, L_{l\neq j}}^{n} \right.$$

$$+ \sum_{\substack{j,k=b \\ j\neq k}}^{n} \left(M_0^j \prod_{\substack{l=b \\ l\neq j,k}}^{n} L \right) / (\tau_{ak}\tau_{ja}) - \sum_{\substack{j,k=b \\ j\neq k}}^{n} \left(M_0^k \prod_{\substack{l=b \\ l\neq j,k}}^{n} L \right) / (\tau_{aj}\tau_{ja}) \qquad \text{(B-2)}$$

$$\left. + \sum_{j=b}^{n} M_0^a \prod_{l=b,\, l\neq j}^{n} L_l / \tau_{aj} \right\} \Big/ \left\{ A \prod_{j=b}^{n} J - \sum_{j=b}^{n} \prod_{l=b,\, l\neq j}^{n} L_l / (\tau_{aj}\tau_{ja}) \right\}$$

Equation (B-2) can be rearranged to put it in the following form.

$$G = -i\,\omega_1 \left\{ M_0^a \left[{}^{(1)}1 + \sum_{j=b}^{n} 1/(\tau_{aj}\, {}^{(2)}J) \right] + \sum_{j=b}^{n} M_0^j / ({}^{(3)}\tau_{ja} J) \right.$$

$$+ \sum_{\substack{j,k=b \\ j\neq k}}^{n} M_0^j / ({}^{(4)}\tau_{ak}\tau_{ja} JK) + \sum_{j=b}^{n} A\, M_0^j / {}^{(5)}J \qquad \text{(B-3)}$$

$$\left. - \sum_{\substack{j,k=b \\ j\neq k}}^{n} M_0^k / ({}^{(6)}\tau_{aj}\tau_{ja} JK) \right\} \Big/ \left\{ A - \sum_{j=b}^{n} 1/(\tau_{aj}\tau_{ja} J) \right\}$$

Each j or k has a J or K associated with it and summations over j and k imply summations over J and K as indicated in Eq. (B-3).

The concentration conditions are such that the concentration of the minor species taken collectively, $\sum_{j=b}^{n} [j]$, is much less than [a]. As a consequence $\sum_{j=b}^{n} M_0^j \ll M_0^a$ as long as M_0^j is essentially determined by j. This will occur when the resonance frequency of the pure j species, ω, satisfies the condition $\sum_{j=b}^{n} \omega_{0j}/\omega_{0a} \leq 1$. Such is the case in the present study. The ratio

$$\sum_{j=b}^{n} M_0^j / M_0^a$$

will be called r.

Another consequence of the concentration conditions is that $\sum_{j=b}^{n} \tau_{ja}/\tau_{aj} = q \ll 1$. One further inequality must be mentioned. In

order to make the derivation coincide with the conditions present in a dilute aqueous solution of paramagnetic ions, something must be said about the ratio of $\Delta\omega_{\underline{j}}$ to $\Delta\omega_{\underline{a}}$. It has been found experimentally that $\Delta\omega_{\underline{j}}$ in the region of interest is on the order of 10^6 sec.$^{-1}$ for all ions studied. The width of the observed resonance signal, approximately equal to the largest value of interest of $\Delta\omega_{\underline{a}}$, is no larger than 10^3 sec.$^{-1}$. Therefore it may be stated that $\Sigma_{\underline{j}=\underline{b}}^{\underline{n}} \Delta\omega_{\underline{a}} / \Delta\omega_{\underline{j}} \ll 1$ and will be referred to as s.

It must also be mentioned that the resonance signal for a solution of interest is appreciably broader than the signal for pure water. Therefore $1/\tau_{\underline{a}} = \Sigma_{\underline{j}=\underline{b}}^{\underline{n}} 1/\tau_{\underline{a}\underline{j}} \gtrsim 1/T_{2\underline{a}}$.

Equation (B-3) may be simplified through an application of these inequalities. It will be shown that for the solutions of interest in this thesis that the term labeled (1) in the numerator of Eq. (B-3) overwhelms the other five. Since there are only five other terms, no matter how large n is, they also do not give an appreciable cumulative effect.

A consequence of the fact that term (1) is the most important term in the numerator of Eq. (B-3) is that $G_{\underline{a}}$ overwhelms $\Sigma_{\underline{j}=\underline{b}}^{\underline{n}} G_{\underline{n}}$. This means that the observed signal arises almost entirely from the nuclei in environment a, broadened and shifted due to their having been in the other n-1 environments. The signals arising from the nuclei in the other n-1 environments are obscured.

Although term (1) is the dominant term under the condition employed in this research, it is not generally so. The following treatment will show that term (1) is the most important under the conditions used here and will also show the conditions necessary for the reversal of this inequality.

The ratio of each of the last five terms to term (1) is taken in order to show it to be of the order of q, r, or s or less. Each ratio is separated into a real and an imaginary component and both parts are shown to be negligible.

One further point must be considered. The ultimate result of this derivation will be the equation of the v component of G. Equation (B-3) for G can be put in the form:

$$G = - i\omega_1 \, (R_1 + i \, I_1) \, / \, (R_2 + i \, I_2)$$

where R_1 and I_1 are the real and imaginary components of the sum of terms in brackets in Eq. (B-3). R_2 and I_2 are the real and imaginary components of the denominator of Eq. (B-3). The v component is

$$v = -\omega_1 \, (R_1 \, R_2 + I_1 \, I_2) \, / \, (R_2^2 + I_2^2)$$

As was stated above, it will be shown that R_1 is essentially the first term in the numerator of Eq. (B-3). Also I_1 will be shown to be much less than R_1. Finally the resultant equation for v will show that I_2 is always $\lesssim R_2$ in the region of interest, so that term (1) is the only term of importance in the numerator of Eq. (B-3).

The following is the detailed consideration of terms.

Term 2

$$\frac{\text{Term 2}}{\text{Term 1}} = \Sigma_{\underline{j}=\underline{b}}^{\underline{n}} \left\{ \frac{1}{\tau_{\underline{a}\underline{j}}(1/T_{2\underline{j}} + 1/\tau_{\underline{j}\underline{a}} - i \, \Delta\omega_{\underline{j}})} \right\}$$

Rationalization of the denominator gives

$$\Sigma_{\underline{j}=\underline{b}}^{\underline{n}} \left\{ \frac{1/T_{2\underline{j}} + 1/\tau_{\underline{j}\underline{a}} + i \, \Delta\omega_{\underline{j}}}{\tau_{\underline{a}\underline{j}} \left[(1/T_{2\underline{j}} + 1/\tau_{\underline{j}\underline{a}})^2 + \Delta\omega_{\underline{j}}^2 \right]} \right\}$$

In consideration of the real part, the sum given above is less than or equal to

$$\sum_{j=b}^{n} \left\{ \frac{1}{\tau_{aj} \left(1/T_{2j} + 1/\tau_{ja}\right)} \right\} \leq q$$

The imaginary part yields

$$\sum_{j=b}^{n} \left\{ \frac{\Delta \omega_j}{\tau_{aj} \left[\left(1/T_{2j} + 1/\tau_{ja}\right)^2 + \Delta \omega_j^2 \right]} \right\}$$

$$= \sum_{j=b}^{n} \left\{ \frac{1}{\left(\tau_{aj}/\Delta \omega_j\right) \left[1/T_{2j}^2 + 2/\left(T_{2j} \tau_{ja}\right) \right] + \tau_{aj}/\left(\tau_{ja}^2 \Delta \omega_j\right) + \tau_{aj} \Delta \omega_j} \right\}$$

$$< \sum_{j=b}^{n} \left\{ \frac{1}{\left(\tau_{aj}/\tau_{ja}\right)^2 \left[1/\left(\tau_{aj} \Delta \omega_j\right) \right] + \tau_{aj} \Delta \omega_j} \right\}$$

The maximum value of the fraction inside the summation occurs when $\tau_{aj} \Delta \omega_j = \tau_{aj}/\tau_{ja}$. Therefore the preceding summation is less than or equal to

$$\sum_{j=b}^{n} 1/\left(2 \tau_{aj}/\tau_{ja}\right) = q/2$$

Thus term (2) may be dropped in comparison to term (1).

Term 3

$$\frac{\text{Term 3}}{\text{Term 1}} = \sum_{j=b}^{n} M_0^j / \left(\tau_{ja} M_0^a J\right)$$

Rationalization of the denominator yields

$$1/M_0^a \sum_{j=b}^{n} \left\{ \frac{M_0^j \left(1/T_{2j} + 1/\tau_{ja} + i\Delta \omega_j\right)}{\tau_{ja} \left[\left(1/T_{2j} + 1/\tau_{ja}\right)^2 + \Delta \omega_j^2 \right]} \right\}$$

To obtain the real component it may be seen that the preceding sum is less than or equal to

$$1/M_0^a \sum_{j=b}^{n} \left\{ \frac{M_0^j (1/T_{2j} + 1/\tau_{ja} + i\Delta\omega_j)}{\tau_{ja} (1/T_{2j} + 1/\tau_{ja})^2} \right\}$$

The real component is

$$1/M_0^a \sum_{j=b}^{n} \frac{M_0^j}{\tau_{ja}(1/T_{2j} + 1/\tau_{ja})} \leq r$$

The imaginary component is obtained in the same manner as that for Term 2/Term 1.

The imaginary component is

$$1/M_0^a \sum_{j=b}^{n} \left\{ \frac{M_0^j \Delta\omega_j}{\tau_{ja} [(1/T_{2j} + 1/\tau_{ja})^2 + \Delta\omega_j^2]} \right\}$$

$$\leq 1/M_0^a \sum_{j=b}^{n} \left\{ \frac{M_0^j}{1/(\tau_{ja}\Delta\omega_j) + \tau_{ja}\Delta\omega_j} \right\}$$

The maximum value of the fraction inside the summation occurs when $\tau_{ja} \Delta\omega_j = 1$. Therefore the preceding summation is less than or equal to

$$1/M_0^a \sum_{j=b}^{n} M_0^j / 2 = r/2$$

Term 3 may be dropped.

Term 4

$$\frac{\text{Term 4}}{\text{Term 1}} = 1/M_0^a \sum_{\substack{j,k=b \\ j\neq k}}^{n} M_0^j / (\tau_{ja}\tau_{ak}\,JK)$$

$$\frac{\text{Term 3}}{\text{Term 1}} \times \frac{\text{Term 2}}{\text{Term 1}}$$

Since Term 3/Term 1 and Term 2/Term 1 are much less than one, the product is also and Term 4 may be dropped.

Terms 5 and 6

Terms 5 and 6 are considered together since they are very similar in form. Also Term 6 is negative and a treatment of the two terms together gives cancellation to produce a positive term.

$$\frac{\text{Term 5 + Term 6}}{\text{Term 1}} = \Sigma_{\underline{j}=\underline{b}}^{\underline{n}} \; A \, M_{\underline{O}}^{\underline{j}} / (M_{\underline{O}}^{\underline{a}} \, J) - \Sigma_{\substack{\underline{j},\underline{k}=\underline{b} \\ j \neq k}}^{\underline{n}} M_{\underline{O}}^{\underline{k}} / (\tau_{\underline{aj}} \tau_{\underline{ja}} \, JK \, M_{\underline{O}}^{\underline{a}})$$

This equation may be expanded and rearranged to yield the following equation.

$$\frac{\text{Term 5 + Term 6}}{\text{Term 1}} = \Sigma_{\underline{k}=\underline{b}}^{\underline{n}} M_{\underline{O}}^{\underline{k}} / (M_{\underline{O}}^{\underline{a}} K) \Big\{ \Big(\Sigma_{\underline{k} \neq \underline{j} = \underline{b}}^{\underline{n}} \, 1/\tau_{\underline{aj}} \Big) + 1/\tau_{\underline{ak}}$$

$$+ 1/T_{2\underline{a}} - i\Delta\omega_{\underline{a}} - \Big[\Sigma_{\underline{k} \neq \underline{j} = \underline{b}}^{\underline{n}} \, 1/(\tau_{\underline{aj}} \tau_{\underline{ja}} \, J) \Big] + 1/(\tau_{\underline{ak}} \tau_{\underline{ka}} \, K)$$

$$- 1/(\tau_{\underline{ak}} \tau_{\underline{ka}} \, K) \Big\}$$

The consideration of this equation is made easier through the elimination of the condition, $j \neq k$, which is present in the summations. This may be accomplished through the demonstration that the term

$$\Sigma_{\underline{k}=\underline{b}}^{\underline{n}} M_{\underline{O}}^{\underline{k}} / (M_{\underline{O}}^{\underline{a}} \, \tau_{\underline{ak}} \tau_{\underline{ka}} K^2)$$

is much less than one. The term is less than Term 3/Term 1 X Term 2/Term 1 and is therefore negligible and will be dropped. The remaining terms yield

$$\sum_{k=b}^{n} M_0^k / M_0^a \left[\frac{1/T_{2k} + 1/\tau_{ka} \pm i\Delta\omega_k}{(1/T_{2k} + 1/\tau_{ka})^2 + \Delta\omega_k^2} \right] \times$$

$$\left[1/T_{2a} - i\Delta\omega_a + \sum_{j=b}^{n} \frac{1/T_{2j}\,(1/T_{2j} + 1/\tau_{ja}) + \Delta\omega_j^2 - i\Delta\omega_j/\tau_{ja}}{\tau_{aj}\left[(1/T_{2j} + 1/\tau_{ja})^2 + \Delta\omega_j^2\right]} \right] \qquad \text{(B-4)}$$

We wish to show that (Term 5 + Term 6)/Term 1 is negligible under the conditions used in this thesis. In order to do this we shall assume that it is of the order of unity or greater and then we shall show that this leads to an absurdity.

If (Term 5 + Term 6)/Term 1 is large, one or more of the signals arising from the n-1 minor environments is visible over the signal arising from environment a or $\sum_{j=b}^{n} G_j \geq G_a$. It is of interest to see just how this can arise from the terms in Eq. (B-4). Therefore these terms must be identified. Consider the equation for G_a.

$$G_a = \frac{-i\omega_1 M_0^a}{A - \sum_{j=b}^{n} 1/(\tau_{aj}\tau_{ja}J)}$$

$$= \frac{-i\omega_1 M_0^a}{1/T_{2a} - i\Delta\omega_a + \sum_{j=b}^{n} \dfrac{1/T_{2j}\,(1/T_{2j} + 1/\tau_{ja}) + \Delta\omega_j^2 - i\Delta\omega_j/\tau_{ja}}{\tau_{aj}\left[(1/T_{2j} + 1/\tau_{ja})^2 + \Delta\omega_j^2\right]}}$$

Therefore the second term in brackets in Eq. (B-4) is for the conditions of interest, $-i\omega_1 M_0^a/G_a$. It will be shown that the real part of $-i\omega_1 M_0^a$ is the half width in radians per second of the v component of the signal G_a at the frequency at which the signal intensity is half its maximum value. The imaginary component will be shown to be the dis-

placement in radians per second of the frequency from the resonance frequency of the observed signal.

(Term 5 + Term 6)/Term 1 when the order of unity or greater is essentially $\Sigma_{\underline{j}=\underline{b}}^{\underline{n}} G_{\underline{j}}/G_{\underline{a}}$. Therefore for such a condition the term

$$\Sigma_{\underline{k}=\underline{b}}^{\underline{n}} M_0^{\underline{k}} (1/T_{2\underline{k}} + 1/\tau_{\underline{ka}} + i\Delta\omega_{\underline{k}})/\left[(1/T_{2\underline{k}} + 1/\tau_{\underline{ka}})^2 + \Delta\omega_{\underline{k}}^2 \right]$$

may be identified as $-1/i\omega_1 \Sigma_{\underline{k}=\underline{b}}^{\underline{n}} G_{\underline{k}}$. This equation may be rearranged to yield

$$\Sigma_{\underline{k}=\underline{b}}^{\underline{n}} G_{\underline{k}} = -i\omega_1 \Sigma_{\underline{k}=\underline{b}}^{\underline{n}} M_0^{\underline{k}} \left[(1/T_{2\underline{k}} + 1/\tau_{\underline{ka}}) + i\Delta\omega_{\underline{k}} \right] /$$

$$\left[(1/T_{2\underline{k}} + 1/\tau_{\underline{ka}})^2 + \Delta\omega_{\underline{k}}^2 \right]$$

The half width at half height of the v compartment of each $G_{\underline{k}}$ which is appreciable with respect to $G_{\underline{a}}$ is thus $1/T_{2\underline{k}} + 1/\tau_{\underline{ka}}$ and the displacement from the pure $\underline{k}$ resonance is, of course, $\Delta\omega_{\underline{k}}$.

Consider the first term of the real component of (Term 5 + Term 6)/Term 1.

$$\Sigma_{\underline{k}=\underline{b}}^{\underline{n}} M_0^{\underline{k}}/M_0^{\underline{a}} \left[\frac{1/T_{2\underline{k}} + 1/\tau_{\underline{ka}}}{(1/T_{2\underline{k}} + 1/\tau_{\underline{ka}})^2 + \Delta\omega_{\underline{k}}^2} \right]$$

$$\left[1/T_{2\underline{a}} + \Sigma_{\underline{j}=\underline{b}}^{\underline{n}} \frac{1/T_{2\underline{j}} (1/T_{2\underline{j}} + 1/\tau_{\underline{ja}}) + \Delta\omega_{\underline{j}}^2}{\tau_{\underline{aj}} \left[(1/T_{2\underline{j}} + 1/\tau_{\underline{ja}})^2 + \Delta\omega_{\underline{j}}^2 \right]} \right]$$

The second term in brackets will be shown to be the half width of the v component of $G_{\underline{a}}$. Experimentally this term is always less than or approximately equal to 10^3 radians per second. In these experiments the frequency was always near that of the pure $\underline{a}$ resonance and all the $\Delta\omega_{\underline{k}}$'s in this frequency region are on the order of 10^6 radians per second.

Since $(1/T_{2\underline{k}} + 1/\tau_{\underline{ka}})/\left[(1/T_{2\underline{k}} + 1/\tau_{\underline{ka}})^2 + \Delta\omega_{\underline{k}}^2\right]$ is less than or equal to $1/\Delta\omega_{\underline{k}}$, the sum given above is much less than one.

For the same reasons given above each of the other terms in the real and imaginary components of (Term 5 + Term 6)/Term 1 are negligible under the conditions employed in this thesis. Terms 5 and 6 may then be dropped.

Equation (B-4) reduces to

$$G = G_{\underline{a}} = \frac{-i\,\omega_1\,M_0^{\underline{a}}}{1/T_{2\underline{a}} - i\Delta\omega_{\underline{a}} + \Sigma_{\underline{j}=\underline{b}}^{\underline{n}} \dfrac{1/T_{2\underline{j}} + 1/\tau_{\underline{ja}}) + \Delta\omega_{\underline{j}}^2 - i\Delta\omega_{\underline{j}}/\tau_{\underline{ja}}}{\tau_{\underline{aj}}\left[(1/T_{2\underline{j}} + 1/\tau_{\underline{ja}})^2 + \Delta\omega_{\underline{j}}^2\right]}}$$

This equation is easily converted to the form, u + iv, yielding the following solution for v.

$$-i\omega_1\,M_0^{\underline{a}}\left[1/T_{2\underline{a}} + \Sigma_{\underline{j}=\underline{b}}^{\underline{n}} \frac{1/T_{2\underline{j}}(1/T_{2\underline{j}} + 1/\tau_{\underline{ja}}) + \Delta\omega_{\underline{j}}^2}{\tau_{\underline{aj}}\left[(1/T_{2\underline{j}} + 1/\tau_{\underline{ja}})^2 + \Delta\omega_{\underline{j}}^2\right]}\right] \tag{B-5}$$

$$v = \frac{}{\left[1/T_{2\underline{a}} + \Sigma_{\underline{j}=\underline{b}}^{\underline{n}} \frac{1/T_{2\underline{j}}(1/T_{2\underline{j}}+1/\tau_{\underline{ja}})+ \Delta\omega_{\underline{j}}^2}{\tau_{\underline{aj}}[(1/T_{2\underline{j}}+ 1/\tau_{\underline{ja}})^2+\Delta\omega_{\underline{j}}^2]}\right]^2 + \left[\Delta\omega_{\underline{a}} + \Sigma_{\underline{j}=\underline{b}}^{\underline{n}} \frac{\Delta\omega_{\underline{j}}}{\tau_{\underline{aj}}\tau_{\underline{ja}}\left[\left(\frac{1}{T_{2\underline{j}}} + \frac{1}{\tau_{\underline{ja}}}\right)^2 + \Delta\omega_{\underline{j}}^2\right]}\right]}$$

As was stated in Part I, Eq. (B-5) is merely Eq. (6) with the summation extended over all the minor components present.

It remains to be shown that the first term in brackets in the denominator of Eq. (B-5) may be identified to a good approximation as the half width at half height. Also it must be shown that the n species extension of Eq. (8) yields the chemical shift.

As was stated previously, from the experimental data it is known that the $\Delta\omega_{\underline{k}}$'s are on the order of 10^6 radians per second. The observed line widths were on the order of 10^3 radians per second. On a

percentage basis the $\Delta\omega_k$'s are virtually constant over the frequency range of interest. The first term in brackets in the denominator of Eq. (B-5) may then be considered to be frequency independent. The maximum value of v occurs when the second term in brackets is equal to zero, so that the chemical shift relative to the maximum of the a resonance line is

$$\Delta\omega_a = -\sum_{j=b}^{n} \frac{\Delta\omega_j}{\tau_{aj}\tau_{ja}[(1/T_{2j} + 1/\tau_{ja})^2 + \Delta\omega_j^2]}$$

The numerator is virtually frequency independent for the same reason given above. Therefore the signal reaches half of its maximum value when the second term in brackets in the denominator equals the first term. The first term in brackets is then a very good approximation to the displacement from resonance in radians per second when the resonance signal has reached half its maximum value.

One further consideration must be made in the application of the results of this derivation to the remarks on the simplification of Eq. (B-3). It was stated that I_2 is always less than or approximately equal to R_2. I_2 has been identified as the displacement in radians per second from the resonance frequency of the observed signal. R_2 is this displacement in radians per second when the signal has reached half its maximum value. I_2 is therefore of no interest past 2 or 3 R_2 and so is always less than or approximately equal to R_2.

It is of interest to investigate Eq. (B-4) under conditions differing from those employed here, i.e., under those conditions which cause it to be large.

The concentration conditions will be the same as previously discussed. The restrictions placed on the $\Delta\omega$'s will be removed however.

For purposes of simplification the sum over $\underline{k}$ will be limited to one particular $\underline{k}$ which must possess a $G_{\underline{k}}$ which is important relative to $G_{\underline{a}}$ What is derived for this $\underline{k}$ would apply equally as well to any other $\underline{k}$ which contributes appreciably to the total signal.

The identification of the restricted first term in brackets in Eq. (B-4) as $-1/(i\,\omega_1)\,[G_{\underline{k}}/\bar{M}_0^{\underline{k}}]$ and the second term in brackets as $-i\,\omega_1\,\bar{M}_0^{\underline{a}}/G_{\underline{a}}$ remains the same. The half width at half height of the v component of $G_{\underline{k}}$ is $(1/T_{2\underline{k}} + 1/\tau_{\underline{ka}})$ and the displacement from the $\underline{k}$ resonance is $\Delta\omega_{\underline{k}}$.

Consider the revised first term of the real component of (Term 5 + Term 6)/Term 1.

$$\bar{M}_0^{\underline{k}} / \bar{M}_0^{\underline{a}} \left[\frac{1/T_{2\underline{k}} + 1/\tau_{\underline{ka}}}{(1/T_{2\underline{k}} + 1/\tau_{\underline{ka}})^2 + \Delta\omega_{\underline{k}}^2} \right] \times$$

$$\left[1/T_{2\underline{a}} + \sum_{\underline{j}=\underline{b}}^{\underline{n}} \frac{1/T_{2\underline{j}}(1/T_{2\underline{j}} + 1/\tau_{\underline{ja}}) + \Delta\omega_{\underline{j}}^2}{\tau_{\underline{aj}} \left[(1/T_{2\underline{j}} + 1/\tau_{\underline{ja}})^2 + \Delta\omega_{\underline{j}}^2 \right]} \right]$$

For large values of $\Delta\omega_{\underline{j}}$ it was shown previously that the second term in brackets is virtually frequency independent.

We wish to now extend that to all values of $\Delta\omega_{\underline{j}}$. Consider the following fraction for one value of $\underline{j}$.

$$\frac{1/T_{2\underline{j}}^2 + 1/(T_{2\underline{j}}\tau_{\underline{ja}}) + \Delta\omega_{\underline{j}}^2}{\tau_{\underline{aj}} \left[(1/T_{2\underline{j}} + 1/\tau_{\underline{ja}})^2 + \Delta\omega_{\underline{j}}^2 \right]}$$

Then consider the possible limiting cases.

(1) $\Delta\omega_{\underline{j}}^2 \gg 1/\tau_{\underline{ja}}^2,\ 1/T_{2\underline{j}}^2$. The fraction reduces to $1/\tau_{\underline{aj}}$ and there is no frequency dependence.

(2) $1/(T_{2\underline{j}}\tau_{\underline{ja}}) \gg 1/\tau_{\underline{ja}}^2, \Delta\omega_{\underline{j}}^2$. The fraction becomes $1/\tau_{\underline{aj}}$ and is again frequency independent.

(3) $1/\tau_{\underline{ja}}^2 \gg 1/(T_{2\underline{j}}\tau_{\underline{ja}}), \Delta\omega_{\underline{j}}^2$. The fraction reduces to $(\tau_{\underline{ja}}/\tau_{\underline{aj}})\, 1/T_{2\underline{j}} + (\tau_{\underline{ja}}/\tau_{\underline{aj}})\Delta\omega_{\underline{j}}^2\, \tau_{\underline{ja}}$. The contribution of the frequency dependent term to the line width equals $(\tau_{\underline{ja}}/\tau_{\underline{aj}})(\Delta\omega_{\underline{j}}\tau_{\underline{ja}})\Delta\omega_{\underline{j}}$. Therefore $\Delta\omega_{\underline{j}}$ is given by the following equation.

$$\Delta\omega_{\underline{j}} = \frac{\text{contribution to the line width from } \underline{j}}{(\tau_{\underline{ja}}/\tau_{\underline{aj}})\,\Delta\omega_{\underline{j}}\,\tau_{\underline{ja}}}$$

$$\gg \text{contribution to the line width from } \underline{j}$$

Therefore $\Delta\omega_{\underline{j}}$ must be essentially constant if it is to be of any importance in the relaxation.

The half width at half height of the v component of the $G_{\underline{a}}$ signal is given by the second term in brackets in the first term of the real component of (Term 5 + Term 6)/ Term 1.

The frequency condition for which the first term in brackets reaches its maximum value is $\Delta\omega_{\underline{k}} = 0$. For this condition the ratio

$$\frac{1/T_{2\underline{a}} + \sum_{\underline{j}=\underline{b}}^{\underline{n}} \dfrac{1/T_{2\underline{j}}\,(1/T_{2\underline{j}} + 1/\tau_{\underline{ja}}) + \Delta\omega_{\underline{j}}^2}{\tau_{\underline{aj}}\left[(1/T_{2\underline{j}} + 1/\tau_{\underline{ja}})^2 + \Delta\omega_{\underline{j}}^2\right]}}{(1/T_{2\underline{k}} + 1/\tau_{\underline{ka}})}$$

must be greater than or equal to r^{-1} if $G_{\underline{k}}$ is to be visible above $G_{\underline{a}}$. The ratio given above is the ratio of the half width at half height of the v component of $G_{\underline{a}}$ to the corresponding value for $G_{\underline{k}}$. Therefore if $\Delta\omega_{\underline{k}}$ and $\Delta\omega_{\underline{a}}$ are both small $G_{\underline{k}}$ is much more narrow than $G_{\underline{a}}$ and appears as a narrow spike in $G_{\underline{a}}$. If $\underline{k}$ is such that $\Delta\omega_{\underline{k}}$ reaches zero

at a frequency far removed from the region of the $G_{\underline{a}}$ resonance, no restriction is necessary on the line width of $G_{\underline{k}}$; however, such a case is of no interest here since it causes no interference with $G_{\underline{a}}$.

The possibility of the spike is inherent in each of the other terms in the real and imaginary components of (Term 5 + Term 6)/Term 1 and it is the only case present which can cause interference with $G_{\underline{a}}$.

FIGURES

1. Cross section of the all-glass sample holder employed in the temperature studies, shown bolted into the NMR probe. Lettered parts are as follows:

   (A) Brass block.
   (B) Brass bolt, welded to probe.
   (C) Rubber gasket.
   (D) Glass coil, 2 mm o.d.
   (E) Nonsilvered Dewar.
   (F) Receiver coil.
   (G) Thermocouple well.
   (H) Solution surface.
   (I) Orifice for filling and evacuating.

2. Dependence on reciprocal of temperature of log T_2 for a 1.82×10^{-4} M solution of $MnSO_4$. Also shown are the temperature dependences of log $T_{1\,exp.}$ and log T_{2H_2O} and log T_{1H_2O}.

3. Temperature dependence of log T_{2p} for a 1.82×10^{-4} M $MnSO_4$ solution with the lines resulting from the curve-fitting.

4. Temperature dependence of log T_{2p} for a 1.00×10^{-3} M $Cu(NO_3)_2$ solution with the lines resulting from the curve-fitting.

5. Temperature dependence of log T_{2p} for a 0.100 M solution of $Ni(NO_3)_2$ at 5.43 Mc. The lines resulting from the curve-fitting process are also shown. Data from 3.39×10^{-2} and 6.12×10^{-3} M solutions were corrected to 0.100 M.

6. Temperature dependence of log T_{2p} of a 0.100 M $Ni(NO_3)_2$ solution. The concentration actually used was 0.200 M but the values were referred to the corresponding value for the more dilute solution for purposes of comparison with Fig. 5. The frequency was 2.00 Mc.

7. Temperature dependence of T_{2p} of $CoSO_4$ and $Co(ClO_4)_2$ solutions at 5.43 mc. and 2.00 mc. The lines resulting from the curve-fitting are also shown. All data are corrected to 1.00×10^{-2} M Co^{+2}.
8. Visible spectrum of a 0.600 M $CoSO_4$ solution at 27°C and 94.5°C. Also shown is the curve representing the difference between the two spectra with the density correction from thermal expansion included.
9. Temperature dependence of log T_{2p} of a 1.44×10^{-2} M $Fe(NH_4)_2(SO_4)_2$ solution at 5.43 mc.
10. Comparison of the rates of water exchange with the rate of replacement of water molecules by sulfate ions in aqueous solutions.
11. Plot of the log of the water exchange rates of the ions studied versus the ionization potential for a d electron in the singly ionized gaseous ion.
12. Plots of the free energy and enthalpy of activation for the exchange of water molecules and the theoretical enthalpies of activation arising from crystal field effects for two possible activated complexes.
13. Logarithmic plot of the water exchange rates versus the first formation constants for the paramagnetic ion-ethylene-diamine system.
14. Logarithmic plot of the water exchange rates versus the third formation constant for the paramagnetic ion-ethylene-diamine system. The Cu^{++} point is only an upper limit.
15. A plot of $P_{Mn}T_{2p}$ for Mn^{+2} solutions from the present O^{17} NMR and from the proton NMR data.[4,12] Also shown are the experimental T_1's obtained in the proton studies. The lines which resulted from the curve - fitting of the O^{17} data are shown, along with the corresponding lines calculated for protons.

16. A plot of $P_{Cu}\ T_{2p}$ for Cu^{+2} solutions, showing O^{17} and proton[4,32] NMR results.

17. A plot of $P_{Ni}\ T_{2p}$ for Ni^{+2} solutions from the O^{17} data and from proton NMR data.[32]

18. A plot of $P_{Co}\ T_{2p}$ for Co^{+2} solutions calculated from O^{17} data and results of proton NMR.[4,32]

19. A plot of $P_{Fe}\ T_{2p}$ for Fe^{+2} solutions using O^{17} and proton[32] data.

BIBLIOGRAPHY

1. R. E. Connick and R. E. Poulson, J. Chem. Phys., 30, 759 (1959).

2. R. E. Connick and E. D. Stover, J. Phys. Chem., 65, 2075 (1961).

3. H. M. McConnell and S. B. Berger, J. Chem. Phys., 27, 230 (1957).

4. R. A. Bernheim, T. H. Brown, H. S. Gutowsky and D. E. Woessner, J. Chem. Phys., 30, 950 (1959).

5. H. M. McConnell, J. Chem. Phys., 28, 430 (1958).

6. Should b or c have its resonance in this region and an extremely long lifetime, G_b or G_c could contribute appreciably to G but over only a very narrow frequency interval. Such conditions were not of interest here.

7. N. Bloembergen, E. M. Purcell, and R. V. Pound, Phys. Rev., 73, 679 (1958).

8. I. Solomon, Phys. Rev., 99, 559 (1955).

9. I. Solomon and N. Bloembergen, J. Chem. Phys., 25, 261 (1956).

10. N. Bloembergen, J. Chem. Phys., 27, 595 (1957).

11. E. E. Genser, Lawrence Radiation Laboratory Report, UCRL 9846, 1961, University of California, Berkeley, California.

12. N. Bloembergen and L. O. Morgan, J. Chem. Phys., 34, 842 (1961).

13. R. S. Codrington and N. Bloembergen, J. Chem. Phys., 29, 600 (1958).

14. M. Tinkham, R. Weinstein, and A. F. Kip, Phys. Rev., 84, 848 (1951).

15. T. S. England and E. E. Schneider, Physica, 17, 221 (1957).

16. R. G. Pearson, J. Palmer, M. M. Anderson and A. L. Allred, Z. fur Electrochem., 64, 110 (1960).

17. C. A. Beevers and H. Lipson, Proc. Roy. Soc., (London), A146, 570 (1933).

18. D. Kivelson, J. Chem. Phys., 33, 1094 (1960).

19. R. G. Hayes, Lawrence Radiation Laboratory Report UCRL 9873, 1961, University of California, Berkeley, California.

20. N. Bloembergen, J. Chem. Phys., 27, 572 (1957).

21. J. A. Jackson, J. F. Lemons, and H. Taube, J. Chem. Phys., 32, 553 (1960).

22. This entropy increase from freeing the two water molecules would be offset to some extent by a closer penetration of water molecules in the second and higher coordination spheres.

23. C. J. Ballhausen, Kgl. Danske Videnskab. Selskab., Mat. - fys. Medd., 29, No. 4 (1954).

24. C. J. Ballhausen and C. K. Jorgensen, Acta Chem. Scand., 9, 397 (1955).

25. M. Eigen, Z. für Electrochem., 64, 115 (1960).

26. M. Eigen, paper contained in "Advances in the Chemistry of the Coordination Compounds", S. Kirschner, Editor, MacMillan, New York, 1961.

27. F. Basolo and R. G. Pearson, "Mechanisms of Inorganic Reactions , Wiley, New York, 1958.

28. C. E. Moore, "Atomic Energy Levels , Circular of the National Bureau of Standards 467, Vol. II, 1952.

29. R. W. G. Wyckoff, "Crystal Structures , Interscience Publishers, Inc., New York, 1948; Table III, 3.

30. J. Bjerrum, "Metal Ammine Formation in Aqueous Solution", P. Haase and Son, Copenhagen, 1941.

31. G. A. Carlson, J. P. McReynolds, and F. H. Verhoek, J. Am. Chem. Soc., 67, 1334 (1945).

32. R. Hausser and G. Laukien, Z. Physik 153, 394 (1959).

33. D. H. Templeton (University of California), private communication.

This report was prepared as an account of Government sponsored work. Neither the United States, nor the Commission, nor any person acting on behalf of the Commission:

A. Makes any warranty or representation, expressed or implied, with respect to the accuracy, completeness, or usefulness of the information contained in this report, or that the use of any information, apparatus, method, or process disclosed in this report may not infringe privately owned rights; or

B. Assumes any liabilities with respect to the use of, or for damages resulting from the use of any information, apparatus, method, or process disclosed in this report.

As used in the above, "person acting on behalf of the Commission" includes any employee or contractor of the Commission, or employee of such contractor, to the extent that such employee or contractor of the Commission, or employee of such contractor prepares, disseminates, or provides access to, any information pursuant to his employment or contract with the Commission, or his employment with such contractor.